NASA TM X- 63060

THE EFFECTS OF THE GALILEAN MOONS
ON JUPITER FLYBY TRAJECTORIES

BERNARD KAUFMAN

SEPTEMBER 1967

GODDARD SPACE FLIGHT CENTER
GREENBELT, MARYLAND

THE EFFECTS OF THE GALILEAN MOONS ON JUPITER FLYBY TRAJECTORIES

Bernard Kaufman

Mission and Systems Analysis Branch
Mission and Trajectory Analysis Division
Goddard Space Flight Center
Greenbelt, Maryland

THE EFFECTS OF THE GALILEAN MOONS ON JUPITER FLYBY TRAJECTORIES

by

Bernard Kaufman

ABSTRACT

The perturbative effects of the four largest moons of Jupiter on a spacecraft that passes close to Jupiter are investigated using a total of twenty different encounter trajectories with the planet. An accurate model for the moons is utilized in the equations of motion which are numerically integrated over the time that the probe spends within Jupiter's sphere of influence. It is shown that the perturbations caused by the moons do have effects on the post encounter heliocentric trajectories which are large enough to make necessary the inclusion of the moons in any detailed study to be undertaken. On the other hand, actual mission objectives such as the time to 10 astronomical units seem to be little affected by the presence of the moons.

A valuable by-product of this study has been the programming of an accurate ephemeris for the Galilean moons which has not previously been available in this country as far as the author has been able to determine.

ACKNOWLEDGEMENTS

CONTENTS

LIST OF TABLES

LIST OF FIGURES

INTRODUCTION

The ultimate goals of deep-space investigations are the understanding of the origin, laws and evolution of our solar system and of the galactic medium itself. By means of a probe to Jupiter and beyond into deep space we may extend our investigations many fold. Such a probe is currently being planned by NASA and will be entering a region never before investigated which will include the asteroid belt and the trapped radiation region at Jupiter.

A probe that is to be sent into deep space requires a tremendous amount of energy which with today's boosters can only be accomplished at the expense of the final payload. An imaginative way around this problem is to use the gravitational attraction of a planet. When a probe is in a free fall trajectory about the sun in such a manner that it passes within the vicinity of a planet, the trajectory is considerably changed by this encounter. The changes must, of course, depend on the encounter geometry of the probe and the planet.

This report considers a probe that will utilize a flyby of the planet Jupiter to obtain changes in the post encounter heliocentric trajectory. A by-product of an encounter with Jupiter is the opportunity to study the planet itself.

Many authors have treated a Jupiter flyby in the past (for example see references 8 thru 13) based on two body motion, however, Jupiter has twelve natural satellites, four of which are rather large and their masses are relatively well known. To the author's knowledge no one has done an integrated trajectory study which includes perturbations by the moons of Jupiter. In this report only the four Galilean moons are included since these are the largest and their masses are well known. The problem of obtaining accurate positions of these moons has resulted in the programming of Sampson's method to generate an ephemeris of the moons. Such a program has not previously been available in this country as far as can be determined.

1

THE TRANSFER TRAJECTORY

The first problem that must be considered is that of the transfer trajectory from the earth to Jupiter. This will involve the determination of the proper launch conditions, parking orbit duration and injection energy to satisfy total flight time and nominal targeting at Jupiter.

Many authors have treated this problem using various methods to obtain a solution. References 1 through 7 in the bibliography give some of these methods and also indicate the complexity of the problem.

Since in the present study we are mainly interested in the probe once it is in the vicinity of Jupiter, the transfer orbit is only of minor interest. For this reason many of the constraints on the trajectory were dropped in order to simplify the solution. An approximate transfer trajectory is obtained using only the flight time and the positions of the launch and target bodies as constraints. No attempt is made to refine the approximate trajectory in any way. The solution of the transfer trajectory under these restrictions is then solved using the well known solution to Lambert's problem. At the target planet the trajectory is altered by using the patched conic assumption which states that at any given time the probe is affected by one and only one body. At any time the gravitational field of a planet is considered to have a force field called the sphere of influence whose radius s is given by (reference 1)

$$S = \left(\frac{m}{M}\right)^{2/5} R_p$$

where m and M are the masses of the planet and sun respectively and R_p is the planet's distance from the sun.

2

During the transfer phase of the probe, the Earth and Jupiter are considered to be massless points until the probe comes within the sphere of influence of Jupiter. The method used to define this conic transfer trajectory is essentially that found in reference 7 and is described below.

Solution of the problem of a transfer trajectory necessitates knowing the heliocentric position vectors of the Earth ($\vec{r}_e$) at launch date and of Jupiter ($\vec{r}_j$) at arrival date. These vectors can be obtained from an ephemeris or by using two body equations and a given position of the planets at some epoch. Figure 1 shows the essential transfer geometry.
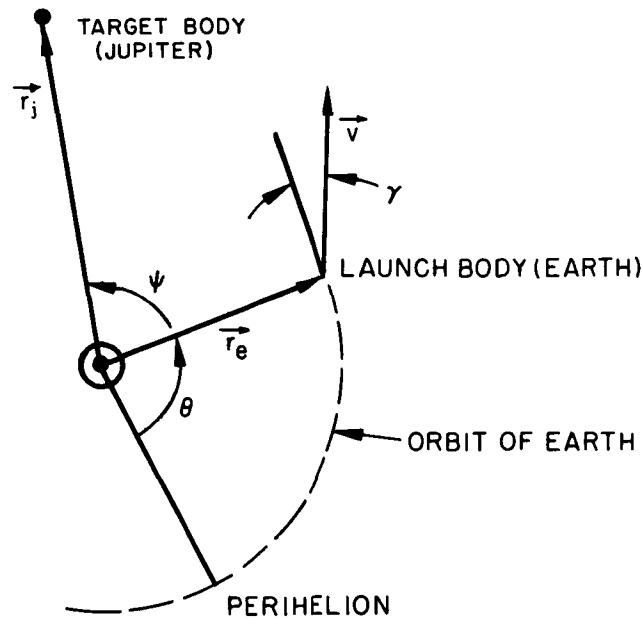
Figure 1—Launch Geometry

The heliocentric transfer angle Ψ in figure 1 can be calculated from $\vec{r}_e$ and $\vec{r}_j$ and is the angle between the position vectors measured in the direction of planetary motion. Two other quantities in figure 1 to be defined are the angles θ and γ. Theta (θ) is the true anomaly of the Earth at launch and γ is the

heliocentric flight path angle which is the angle between a perpendicular to $\vec{r}_e$ and the velocity vector $\vec{v}$ of the probe at launch. The angle γ is the parameter that we wish to calculate.

In order that the launch body and target body lie on a single conic orbit it is necessary that the following be true

$$r_e = \frac{\rho}{1 + e \cos \theta} \tag{1}$$

$$r_j = \frac{\rho}{1 + e \cos (\theta + \Psi)} \tag{2}$$

where $\rho = a(1-e^2)$ is the semi latus rectum.

From (2)

$$\rho = r_j \left[1 + e \cos \theta \cos \Psi - e \sin \theta \sin \Psi\right] \tag{3}$$

and from (1)

$$e \cos \theta = \left(\frac{\rho}{r_e} - 1\right) \tag{4}$$

From figure (1)

$$Tan \gamma = \cot (90 - \gamma) = \frac{\vec{r}_e \cdot \vec{v}}{|\vec{r}_e \times \vec{v}|}$$

$$= \frac{\vec{r}_e \cdot \vec{v}}{\sqrt{a(1 - e^2)}}$$

$$= \frac{e \sin E}{\sqrt{1 - e^2}} = \frac{r_e \, e \sin \theta}{\rho}$$

Therefore

$$e \sin \theta = \frac{\rho}{r_e} Tan \gamma \tag{5}$$

substituting (4) and (5) into (3) we obtain

$$\rho = \frac{r_e \, r_j \, (1 - \cos \Psi)}{r_e - r_j \cos \Psi + r_j \sin \Psi \, Tan \gamma} \tag{6}$$

Equation 6 characterizes the conic section connecting the two radius vectors and it is obvious that ρ is a function only of the unknown angle γ.

The calculation of γ is an interative procedure and only one value of γ will yield the desired flight time between the two planets. Reference to figure 2 shows that two transfer trajectories of very short time exist. One is the straight line solution and the other bends very close around the sun (hot line). A solution lying inside the triangle formed by these two is forbidden since no conic section with the sun at a focus exists in this region. Thus a lower limit (γ_{min}) can be calculated for γ by using the straight line solution and it is easily seen that

$$\gamma_{min} = \mathrm{Tan}^{-1}\left[\frac{r_j \cos \Psi - r_e}{r_j \sin \Psi}\right] \tag{7}$$

The second limit for γ is that for a posigrade parabolic orbit for an infinite transfer time. Reference to figure 3 shows the typical geometry for this orbit.
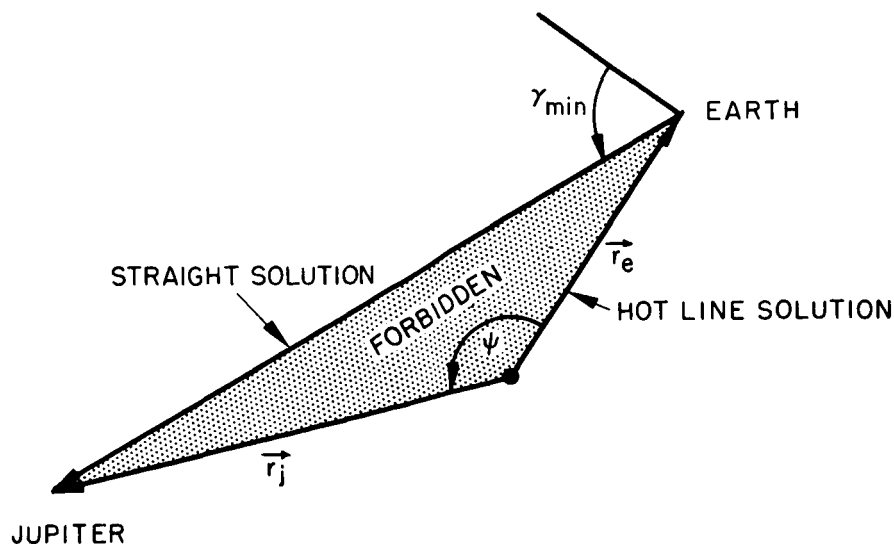
Figure 2—First Limit for Launch Trajectories
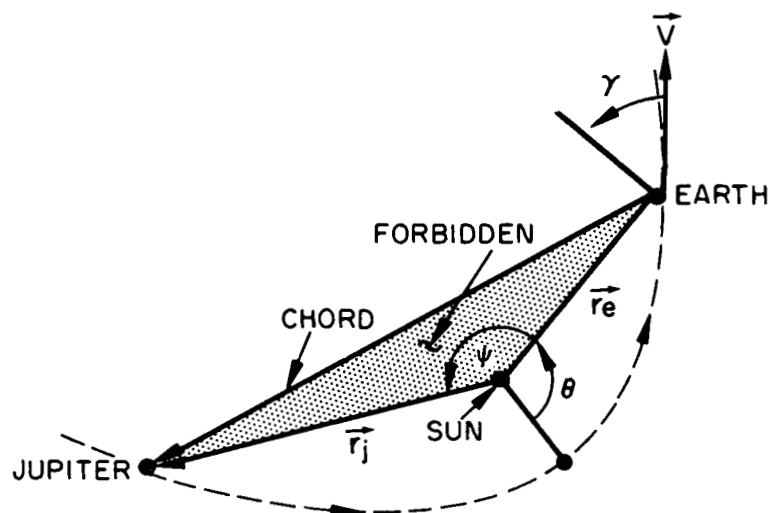
Figure 3—Second Limit for Launch Trajectories

Recall equation (5)

$$e \sin \theta = \frac{\rho}{r_e} \operatorname{Tan} \gamma$$

but for this orbit e = 1 and

$$\rho = \frac{2r}{1 + \operatorname{Tan}^2 \frac{\theta}{2}}$$

Therefore

$$\sin \frac{\theta}{2} \cos \frac{\theta}{2} = \frac{\operatorname{Tan} \gamma}{\dfrac{\cos^2 \frac{\theta}{2} + \sin^2 \frac{\theta}{2}}{\cos^2 \frac{\theta}{2}}}$$

$$= \cos^2 \frac{\theta}{2} \operatorname{Tan} \gamma$$

or

$$\operatorname{Tan} \frac{\theta}{2} = \operatorname{Tan} \gamma$$

Therefore for a parabola

$$\theta = 2\gamma \tag{8}$$

From equations (1) and (2) we have

$$r_e (1 + \cos\theta) = r_j [1 + \cos(\theta + \Psi)]$$

or

$$r_e - r_j = (r_j \cos\Psi - r_e) \cos\theta - (r_j \sin\Psi) \sin\theta$$

where θ is to be eliminated.

The square root of the sum of the squares of the coefficients of θ is:

$$(r_j^2 + r_e^2 - 2r_e r_j \cos\Psi)^{1/2} = \text{chord}$$

thus

$$\frac{r_e - r_j}{\text{chord}} = \cos\alpha \cos\theta - \sin\alpha \sin\theta$$

where

$$\left. \begin{array}{l} \cos\alpha = \dfrac{r_j \cos\Psi - r_e}{\text{chord}} \\[4mm] \sin\alpha = \dfrac{r_j \sin\Psi}{\text{chord}} \end{array} \right\} \tag{9}$$

Thus

$$\frac{r_e - r_j}{\text{chord}} = \cos(\alpha + \theta) = \cos\beta$$

and α can be evaluated from eqn (9)

$$\alpha = \text{Tan}^{-1}\left[\frac{r_j \sin\Psi}{r_j \cos\Psi - r_e} \right]$$

Therefore

$$\alpha + \theta = \beta$$

and from (8)

$$\theta = 2\,\gamma.$$

Thus

$$\gamma_{\text{LIM}} = \frac{\beta - \alpha}{2} \qquad\qquad (10)$$

Equations (7) and (10) now allow us to compute the transfer trajectory in the following manner:*

the initial guess for γ is

$$\gamma_i = \begin{cases} \gamma_{\min} & \text{if } \Psi < 180° \\[2ex] -\pi/2 & \text{if } \Psi > 180° \end{cases}$$

and a step size (ss) for γ_i is chosen such that

$$\gamma_n = \gamma_{n-1} + \text{SS}$$

and

$$\gamma_{\min} < \gamma_n < \gamma_{\lim}$$

From eqn (6)

$$\rho = \frac{r_e\, r_j\, (1 - \cos\Psi)}{r_j\, \sin\Psi\, \text{Tan}\,\gamma_n - r_j\, \cos\Psi + r_e}$$

The velocity is given by

$$v^2 = \frac{2\mu_s}{r_e} - \frac{\mu_s}{a}$$

$$= \frac{\rho\mu_s}{r_e^2\, \cos^2\gamma_n}$$

where μ_s is the gravitational constant of the sun.

---

*These two limits on γ also rule out retrograde transfer orbits

Define

$$C3 = v^2 - \frac{2\mu_s}{r_e} = -\frac{\mu_s}{\alpha}$$

which is twice the total energy per unit mass.

It can easily be shown that

$$e \sin \theta = v \sin \gamma_n \sqrt{\frac{\rho}{\mu_s}}$$

which yields θ .

Then

$$a = -\frac{\mu_s}{C3}$$

$$e = \left(1 - \frac{\rho}{a}\right)^{1/2}$$

Appendix A shows how the time (t_e) from periapsis to a true anomaly of θ can be calculated. In a similar manner the time (t_j) from periapsis to Jupiter can be calculated. Then the flight time is

$$\Delta t = t_j - t_e .$$

If Δt is within a predetermined tolerance to the desired flight time then nothing more need be done. If not, the method of false position allows an iterative solution to γ for the desired flight time. The quantities finally obtained are v, a, e, θ and γ .

Using the above calculated γ we may calculate the velocity vector $\vec{v}$ by decomposing onto two unit vectors $\vec{r}_e^{\,0}$ and $(\vec{r}_e \times \vec{r}_j)^0 \times \vec{r}_e^{\,0}$ as in figure 4. We obtain

$$\vec{v} = \frac{v}{r_e} \left[\cos \gamma \, (\vec{r}_e \times \vec{r}_j)^0 \times \vec{r}_e + \sin \gamma \, \vec{r}_e \right] \tag{11}$$
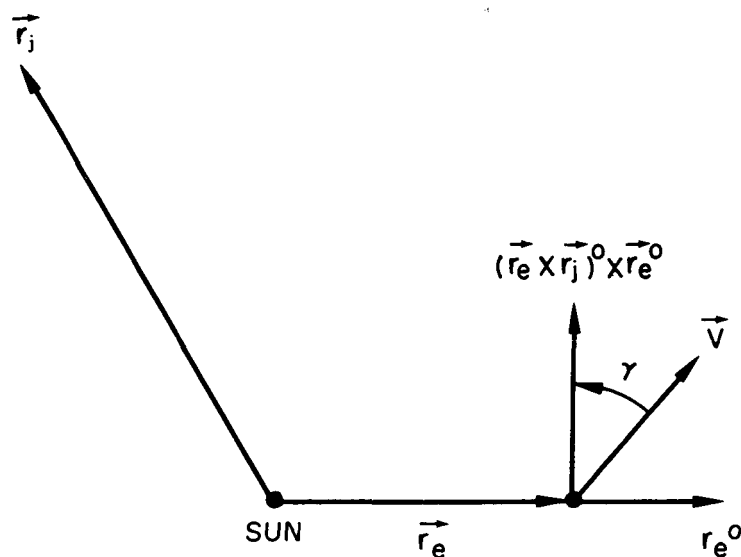
Figure 4—Launch Velocity Diagram

Equation 11 represents the velocity vector of the probe when it is launched from the Earth towards Jupiter. This velocity vector along with Ψ, the heliocentric transfer angle, and the position vector of the probe is all that is necessary to find the position and velocity of the probe at arrival at Jupiter. It is easily seen that for this approximate transfer trajectory, the position vector of the probe at launch is that of the Earth which is obtainable from the ephemeris. Appendix B describes the method used to update the position and velocity of the probe to the arrival date at Jupiter.

UNDISTURBED JUPITER FLYBY AND POST ENCOUNTER TRAJECTORY

The Sphere of Influence

As discussed in the last section the heliocentric velocity vector of the transfer orbit can be obtained at the arrival date at Jupiter. Since in this approximate scheme Jupiter is considered to be a massless point this arrival date is actually an impact time. The problem now is to determine the position and velocity of the probe at arrival at the sphere of influence of Jupiter. The heliocentric position vector of the probe at impact is obviously that of Jupiter.

Using the equation for the radius of the sphere of influence (S) discussed earlier

$$S = \left(\frac{m}{M}\right)^{2/5} R_p$$

the method of false position and two body equations allows us to back up the $\vec{r}$ and $\vec{v}$ from impact to a distance S and thus obtain $\vec{r}$ and $\vec{v}$ at entrance to the sphere of influence.

We let $\vec{r}$ and $\vec{v}$ be the heliocentric impact position and velocity. From $\vec{r}$ and $\vec{v}$ we can easily compute the semi-major axis a, the eccentricity e, the mean motion n and the true anomaly θ_i at impact. From θ_i we find the eccentric anomaly E from

$$\left. \begin{array}{l} \mathrm{Sin}\, E = \dfrac{\sqrt{1 - e^2}\, \sin \theta_i}{1 + e \cos \theta_i} \\[4mm] \mathrm{Cos}\, E = \dfrac{\cos \theta_i + e}{1 + e \cos \theta_i} \end{array} \right\} \qquad (12)$$

11

Kepler's equation then allows us to compute the time t_i from periapsis to θ_i

$$M = E - e \sin E = n t_i \tag{13}$$

The next step is to start the false position interation by choosing a time

$$t = t_i - \Delta t_n \tag{14}$$

where Δt_n can be any arbitrary time.

Kepler's equation is then solved for E in an interative procedure as

$$E_n = M + e \sin E_{n-1} \tag{15}$$

where $E_o = M$ and $M = n t$

The true anomaly θ at time t is then found from

$$\left. \begin{array}{l} \sin \theta = \dfrac{\sqrt{1 - e^2} \, \sin E}{1 - e \cos E} \\[4mm] \cos \theta = \dfrac{\cos E - e}{1 - e \cos E} \end{array} \right\} \tag{16}$$

We now have $\delta = \theta_i - \theta$ and using the procedure in Appendix B we may find $\vec{r}_n, \vec{v}_n$ the position and velocity at time t.

Define a function F

$$F = D - S \tag{17}$$

where D is the distance from Jupiter which is obtained from $\vec{r}_n$ and the ephemeris of Jupiter. A new Δt_{n+1} is then calculated from

$$\Delta t_{n+1} = \frac{\Delta t_{n-1} F_n - \Delta t_n F_{n-1}}{F_n - F_{n-1}} \tag{18}$$

where of course at the beginning

$$\Delta t_0 = 0$$

and

$$F_{n-1} = -S.$$

We then return to equation (14) and repeat the procedure until the function F is within a predetermined small value.

The Undisturbed Post Encounter Trajectory

We have now determined the heliocentric position and velocity $\vec{r}$ and $\vec{v}$ of the probe when it enters Jupiter's sphere of influence. The next problem is to find the post encounter orbit of the probe after it has passed thru the sphere of influence as a function of encounter geometry. References 8 thru 13 describes various methods used to obtain the post encounter orbit as a function of encounter conditions. The method described below is that used by the authors of references 8 and 9 with some modification to make the method more accurate.

We have $\vec{v}$ from above and knowing the injection date of the probe and the time to the sphere of influence we can find $\vec{v}_p$ the heliocentric velocity of Jupiter from the ephemeris data. The velocity of the probe with respect to Jupiter at entrance to the sphere of influence, $\vec{v}_1'$, is then given by

$$\vec{v}_1' = \vec{v} - \vec{v}_p$$

as can be seen from a diagram of the velocity vectors.

Within the sphere of influence the probe's trajectory will be hyperbolic with respect to the planet (reference 1 — see figure 5). We assume that we may choose the radius of closest approach r_p of the probe without significantly altering the direction or magnitude of $\vec{v}_1'$. This is equivalent to assuming that while the direction and magnitude of $\vec{v}_1'$ are fixed at the calculated values, we are still free to choose the point at which the probe pierces the surface of the sphere of influence (point A in figure 5). That this assumption is valid is indicated by Table 1 (from reference 8) where $\vec{v}_1'$ lies along the $\vec{S}^\circ$ vector (figure 5). This table was compiled for both retrograde and posigrade flybys of Jupiter and for a radius of closest approach r_p varying from 100,000 to 10,000,000 km. These values for r_p span a far larger region than we are interested in.
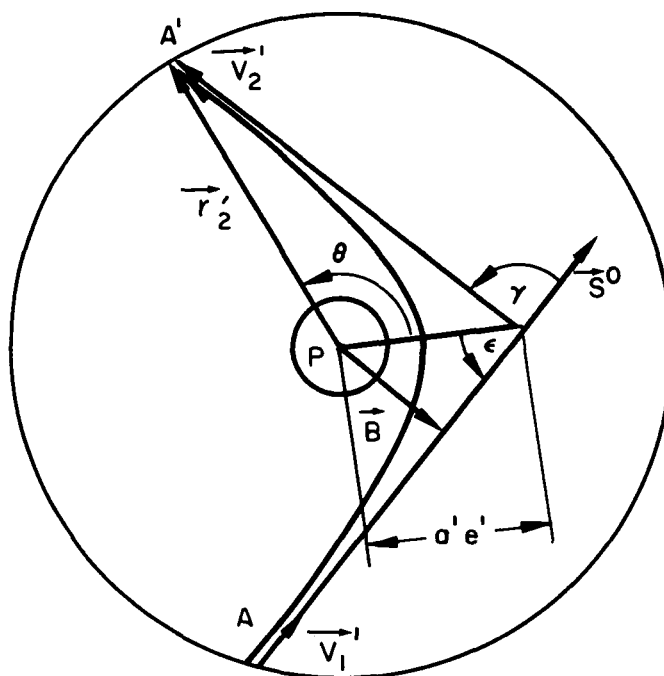
Figure 5—Encounter Orbit Within the Sphere of Influence
(From Reference 8)

For a given asymptote and energy at entrance it will be shown that the entire trajectory within the sphere of influence, including r_p, is determined by the location of point A.

A convenient method for specifying the location of point A (reference 8, 9 and 11) and the radius of closest approach is to select the magnitude of the miss vector ($|\vec{B}|$ = B in figure 5) and an angle Ψ, measured between $\vec{B}$ and a fixed vector in the planet's orbital plane. This fixed vector $\vec{T}^{\circ}$ is one axis of an orthogonal coordinate system whose origin is the planet's center and consists of the unit vectors $\vec{S}^{\circ}$, $\vec{T}^{\circ}$ and $\vec{R}^{\circ}$ (References 10, 11, 14 and 15). These vectors can be defined in the following manner:

$$\vec{S}^{\circ} = \frac{\vec{v}_1'}{|\vec{v}_1'|}$$

Table I

The Velocity Vector as a Function of Choosing the Entrance
Point on the Sphere of Influence (from reference 8)

Posigrade $r_p \times 10^5$ km	$\vec{S}°$		$|\vec{V}_1|$ (km/sec)
	Right Ascension (DEG)	Declination (DEG)	
1	161.38295	-.037895218	13.863505
5	161.36287	-.037826118	13.873625
10	161.34038	-.037764311	13.882193
50	161.10998	-.037458739	13.910651
100	160.75975	-.037179910	13.922712
Retrograde			
1	161.43148	-.037922481	13.863560
5	161.48549	-.037896001	13.873828
10	161.53529	-.037877017	13.882264
50	161.82623	-.037871506	13.910774
100	162.11483	-.037958746	13.923062

$\vec{S}°$ is assumed to lie along the incoming asymptote of the hyperbola;

$$\vec{T}° = \vec{k}° \times \vec{S}°$$

where $\vec{k}°$ is a unit vector perpendicular to the planet's orbital plane;

$$\vec{R}° = \vec{S}° \times \vec{T}°.$$

The vector $\vec{T}°$ lies in the planet's orbital plane and is positive in the direction of the planet's motion. We define Ψ to be the angle between $\vec{T}°$ and $\vec{B}$ measured in the direction $\vec{T}°$ to $\vec{R}°$. Figure 6 (From ref. 14) shows the geometry of this coordinate system and its relationship to the impact plane which is perpendicular to the incoming asymptote.
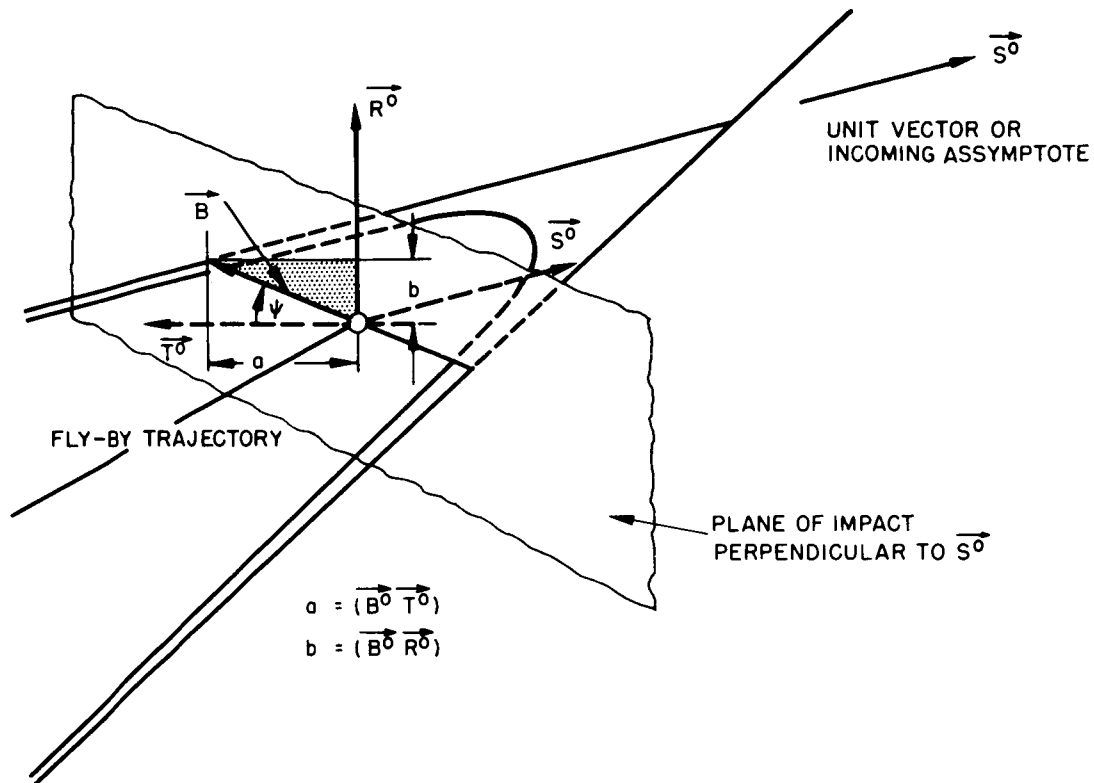
Figure 6—Planetary Approach Coordinate System and Impact Plane (From Reference 14)

The total effect of the undisturbed encounter is simply to rotate $\vec{v}'_1$, thru an angle γ, as illustrated in figure 5, since we must have

$$|\vec{v}'_1| = |\vec{v}'_2|$$

if energy is to be conserved (references 1, 8 and 11). We may easily calculate γ if B is specified:

let a be the semi major axis of the hyperbolic orbit. Then from a straight forward rearrangement of the energy equation we have

$$a = \frac{\mu_p\, S}{2\mu_p - S\,|\vec{v}'_1|^{\,2}} \tag{19}$$

where μ_p is the planet's gravitational constant. From figure 5 and the properties of an hyperbola we have the eccentricity

$$e = \frac{1}{\cos \epsilon} \qquad (20)$$

where ϵ is the half angle between the asymptotes and

$$\sin \epsilon = \frac{|\vec{B}|}{ae} = \frac{B}{a} \cos \epsilon .$$

Therefore

$$\text{Tan } \epsilon = \frac{B}{a} \qquad (21)$$

now

$$\gamma = \pi - 2\epsilon \qquad \text{or}$$

$$\gamma = \pi - 2 \text{ Tan}^{-1} \left(\frac{B}{a} \right) \qquad (22)$$

and the radius of closest approach is

$$r_p = a(1 - e). \qquad (23)$$

We have already pointed out how we may choose the point of entry on the sphere of influence without altering the direction or magnitude of $\vec{v}'_1$. However, this obviously will change $\vec{r}'_1$ the Jovian centered position vector of the probe. We have shown how the parameters B and Ψ define the entrance point on the sphere of influence and allow the calculation of the hyperbolic orbit. We can use B and Ψ to obtain $\vec{r}'_1$ from which we will then be able to easily calculate the post encounter orbit at exit from the sphere of influence. We will also use $\vec{v}'_1$ and the resulting $\vec{r}'_1$ as starting conditions for the calculation of the disturbed orbit in the next section.

Figure 7 shows the relationship of the vectors and angles involved in the $\vec{R}^\circ$, $\vec{S}^\circ$, $\vec{T}^\circ$ coordinate system.
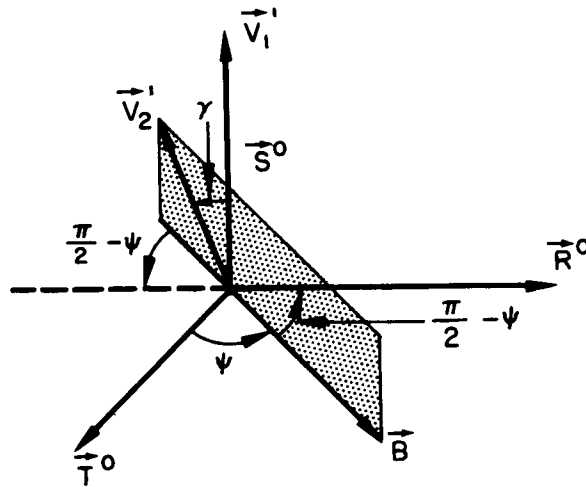
Figure 7—Relationships in the Approach Coordinate
System (From Reference 8)

Referring to this figure we see that

$$\vec{B}° = \vec{T}° \cos \Psi + \vec{R}° \sin \Psi$$

From equations (19) and (20) we find the semi latus rectum

$$\rho = |a (e^2 - 1)| \tag{24}$$

and the true anomaly at entrance to the sphere of influence

$$\theta = \cos^{-1} \frac{\rho - S}{Se} \tag{25}$$

Now from figure 5 we find $\vec{r}'_1$, the Jovian centered position vector at entrance
to the sphere of influence

$$\vec{r}'_1 = S [\cos (\theta + \epsilon - \pi/2) \vec{B}° + \cos (\theta + \epsilon) \vec{S}°] \tag{26}$$

Equation (26) however does not represent the true position vector since it was
assumed that $\vec{v}'_1$ represents the incoming asymptote

$$\vec{S}° = \frac{\vec{v}'_1}{|\vec{v}'_1|}$$

$\vec{S}°$ is therefore not the true asymptote and the miss vector $\vec{B}$ is not quite perpendicular to $\vec{S}°$. The position vector $\vec{r}_1'$ is thus not quite compatible with the anomaly θ. We may make the entire orbit compatible by using $\vec{r}_1'$ to calculate a new θ and a new time in the sphere of influence as follows:

the semi latus rectum is

$$\rho = \frac{|\vec{r}_1' \times \vec{v}_1'|^2}{\mu_p}$$

then

$$C3 = |\vec{v}_1'|^2 - \frac{2\mu_p}{r_1'}$$

$$a = -\frac{\mu_p}{C3}$$

$$e = \sqrt{1 + \frac{C3\,\rho}{\mu_p}}$$

and finally

$$\theta = \cos^{-1}\left(\frac{\rho - r_1'}{r_1'\, e}\right).$$

The procedure in Appendix A then yields the time from perijove to the sphere of influence which is one half the total time spent in the sphere. The differences in total time spent in the sphere of influence between this new trajectory and the approximate trajectory is on the order of 10 minutes when the total time is approximately 80 days and the magnitude B of the miss vector changes by less than one percent. Since B was one of the parameters which define the en-counter orbit and therefore is chosen beforehand, any change in B will slightly alter the encounter trajectory. But since the change in B is small any changes produced by making the orbit consistent with $\vec{r}_1'$ are negligible. Table 2 shows the differences, resulting from this procedure, obtained in the magnitude of the miss vector and the total time in the sphere of influence.

Table II

Effects of Approximating the Encounter Trajectory

ψ	Old B (km)	New B (km)	Δ (km)	Old Time (days)	New Time (days)	Δ (days)
180°	1.25×10^6	1.26×10^6	$.01 \times 10^6$	83.009384	83.017077	.0077
0°	1.25×10^6	1.26×10^6	$.01 \times 10^6$	83.009384	83.017128	.0077
180°	1.0×10^6	1.0078×10^6	$.0078 \times 10^6$	81.453790	81.460214	.0064
0°	1.0×10^6	1.0078×10^6	$.0078 \times 10^6$	81.453790	81.460217	.0064
180°	5.0×10^6	5.0389×10^6	$.0389 \times 10^6$	82.912777	82.915892	.0031
0°	5.0×10^6	5.0388×10^6	$.0388 \times 10^6$	82.912777	82.915926	.0031

With the now determined Jovian centered position and velocity $\vec{r}_1'$ and $\vec{v}_1'$ and the total time t spent in the sphere of influence we are in a position to find $\vec{r}_2'$ and $\vec{v}_2'$ the Jovian centered position and velocity of the probe at exit from the sphere (Point A' in figure 5). To do this one needs an accurate means of stepping along the hyperbola. The method used to determine $\vec{r}_2'$ and $\vec{v}_2'$ is described fully in Appendix C.

Using t the time in the sphere of influence we can determine the position and velocity of Jupiter from ephemeris information at the time the probe leaves the sphere of influence. This position and velocity with $\vec{r}_2'$ and $\vec{V}_2'$ determines the heliocentric position and velocity of the post encounter trajectory.

THE PERTURBED JUPITER FLYBY

As pointed out in the previous section the Jovian centered $\vec{r}\,'_1$ and $\vec{v}\,'_1$ obtained there are also to be used as starting conditions for the disturbed trajectory. The disturbed trajectory is treated in the standard manner using either Cowell's or Encke's method. A review of these methods is given below.

Cowell's Equations of Motion — Perturbations in Rectangular Coordinates

Figure 8 shows three bodies, S , P and P' with masses M , m and m' respectively. The point 0 is a fixed point in space. We consider P to be the body which is in motion about S and is disturbed by body P' .
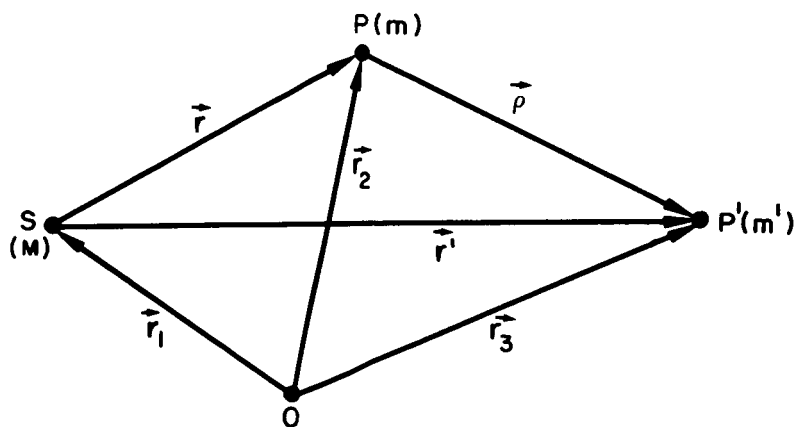

Figure 8—Vector Diagram of Cowell's Equations

Referring everything to point 0 we may express the force on S as

$$M \frac{d^2 \vec{r}_1}{dt^2} = \frac{k^2 M m}{|\vec{r}_1 - \vec{r}_2|^3} (\vec{r}_2 - \vec{r}_1) + \frac{k^2 M m'}{|\vec{r}_1 - \vec{r}_3|^3} (\vec{r}_3 - \vec{r}_1) \qquad (27)$$

The force on P is

$$\frac{m d^2 \vec{r}_2}{dt^2} = \frac{k^2 M m}{|\vec{r}_2 - \vec{r}_1|^3} (\vec{r}_1 - \vec{r}_2) + \frac{k^2 m m'}{|\vec{r}_3 - \vec{r}_2|^3} (\vec{r}_3 - \vec{r}_2) \qquad (28)$$

we define

$$\vec{r} = \vec{r}_2 - \vec{r}_1$$

$$\vec{r}' = \vec{r}_3 - \vec{r}_1$$

$$\vec{r}' - \vec{r} = \vec{r}_3 - \vec{r}_2 = \vec{\rho}$$

By subtracting equation (27) from (28) and making the above substitutions we obtain

$$\frac{d^2 \vec{r}}{dt^2} = -\frac{k^2 (M + m)}{r^3} \vec{r} + k^2 m' \left(\frac{\vec{r}' - \vec{r}}{\rho^3} - \frac{\vec{r}'}{r'^3} \right) \qquad (29)$$

This is Cowell's equation of motion in rectangular coordinates and is now referenced to the central body S. If there is more than one disturbing body the above equation may be written as:

$$\frac{d^2 \vec{r}}{dt^2} = -\frac{k^2 (M + m)}{r^3} \vec{r} + \sum_i k^2 m_i' \left(\frac{\vec{r}_i' - \vec{r}}{\rho_i^3} - \frac{\vec{r}_i'}{r_i'^3} \right) \qquad (30)$$

Encke's Equations of Motion

In the above development if the acceleration due to the disturbing bodies is of the same or higher order as that due to the central force field then Cowell's procedure is a good one to use (reference 1). If, however, the disturbing acceleration is small then Cowell's method becomes inefficient. If in this case

only the differential accelerations are integrated then efficiency and accuracy may be retained. This procedure is the well-known Encke's method.

Define

$$\vec{r} = \vec{r}_0 + \delta \vec{r}$$

where $\vec{r}_0$ is the two body position vector and $\delta\vec{r}$ is the differential correction. The equation of motion is then

$$\frac{d^2\vec{r}}{dt^2} = -\frac{k^2 M \vec{r}}{r^3} + \vec{F} \qquad (31)$$

where $\vec{F}$ is the disturbing acceleration.

For the two body case we have

$$\frac{d^2\vec{r}_0}{dt^2} = -\frac{k^2 M \vec{r}_0}{r_0^3} \qquad (32)$$

Upon subtracting (32) from (31) we obtain

$$\frac{d^2 \delta \vec{r}}{dt^2} = -\frac{k^2 M \delta \vec{r}}{r_0^3} + k^2 M \left(\frac{1}{r_0^3} - \frac{1}{r^3} \right) \vec{r} + \vec{F} \qquad (33)$$

Denote

$$\frac{k^2 M}{r_0^3} = h \qquad (34)$$

and

$$\frac{r^2}{r_0^2} = 1 + 2q$$

Observe that since r^2 and r_0^2 are nearly equal, $2q$ will be small.

Now

$$1 + 2q = \frac{\vec{r} \cdot \vec{r}}{r_0^2} = \frac{(\vec{r}_0 + \delta\vec{r}) \cdot (\vec{r}_0 + \delta\vec{r})}{r_0^2}$$

$$= \frac{r_0^2 + 2\vec{r}_0 \cdot \delta\vec{r} + \delta\vec{r} \cdot \delta\vec{r}}{r_0^2} .$$

Therefore

$$q = \frac{(\vec{r}_0 + 1/2\, \delta\vec{r}) \cdot \delta\vec{r}}{r_0^2} \tag{35}$$

and

$$\frac{r_0^3}{r^3} = (1 + 2q)^{-3/2} \tag{36}$$

Then equation (33) becomes upon substituting (34) and (36)

$$\frac{d^2\delta\vec{r}}{dt^2} = -h\delta\vec{r} + h\,[1 - (1 + 2q)^{-3/2}]\,\vec{r} + \vec{F} \tag{37}$$

Observe that

$$1 - (1 + 2q)^{-3/2} = q\left(3 - \frac{15}{2}q + \cdots\right) = fq$$

then

$$\frac{d^2\delta\vec{r}}{dt^2} = -h\delta\vec{r} + hfq\vec{r} + \vec{F} \tag{38}$$

Equation (38) is the form of Encke's equations used for computation. However, Encke's equations do have a disadvantage that causes computation time to increase. When the magnitude of $\delta\vec{r}$ in equation (38) becomes large it is necessary to change the two body vector $\vec{r}_0$ by defining $\vec{r}_0 = \vec{r}$ if accuracy is to be maintained. This process, known as rectification, requires the numerical integrator to be restarted with a resulting increase in time. It should be pointed out that the disturbing acceleration $\vec{F}$ is the same as in equation (30) above; i.e.,

$$\vec{F} = \sum_i k^2 m_i' \left(\frac{\vec{r}_i' - \vec{r}}{\rho_i^3} - \frac{\vec{r}_i'}{r_i'^3}\right) \tag{39}$$

and that the only change has been in the central body term of equation (30).

Perturbations Due to the Sun

In the above equation (39) for the disturbing acceleration we will include only the four great moons of Jupiter. Since the distance of the sun from Jupiter is so much larger than that of the moons, the term in parentheses in equation (39) for the sun will lose accuracy because of the fact that both members are almost equal. We may eliminate this problem in a manner similar to Encke's procedure by treating the sun as a special case. Reference 16 describes a method for solving this problem and the procedure is repeated below.
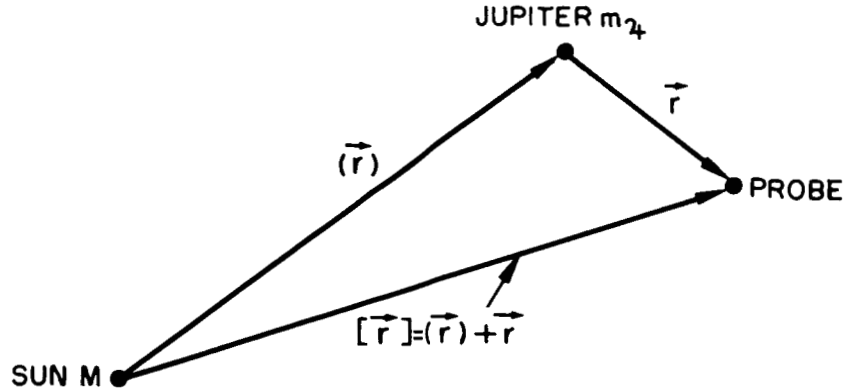

Figure 9—Vector Diagram of Sun, Jupiter and Probe

Figure 9 shows the geometry of the sun, Jupiter and Probe during the encounter phase. By a slight change in notation we may write equation (29) for the case where Jupiter is the central body and the sun is the disturbing body:

$$\frac{d^2\vec{r}}{dt^2} = - \frac{k^2 m_{\scriptscriptstyle\textrm{24}}}{r^3} \vec{r} + k^2 M \left(\frac{-(\vec{r}) - \vec{r}}{|(\vec{r}) + \vec{r}|^3} - \frac{-(\vec{r})}{|(\vec{r})|^3} \right)$$

or

$$\frac{d^2\vec{r}}{dt^2} = - \frac{k^2 m_{\scriptscriptstyle\textrm{24}}}{r^3} \vec{r} - k^2 M \left(\frac{(\vec{r}) + \vec{r}}{|(\vec{r}) + \vec{r}|^3} - \frac{(\vec{r})}{|(\vec{r})|^3} \right) \tag{40}$$

where $\vec{r}$ and $(\vec{r})$ are defined as in figure 9 and the notational change is obvious by comparing figures 8 and 9.

Now

$$|(\vec{r}) + \vec{r}|^2 = |(\vec{r})|^2 + 2(\vec{r}) \cdot \vec{r} + |\vec{r}|^2 \tag{41}$$

let

$$q = \frac{\frac{1}{2}r^2 + (\vec{r}) \cdot \vec{r}}{|(\vec{r})|^2} \tag{42}$$

then

$$2|(\vec{r})|^2 q = r^2 + 2(\vec{r}) \cdot \vec{r}$$

upon substituting this into equation (41) we obtain

$$|(\vec{r}) + \vec{r}|^2 = |(\vec{r})|^2 + 2|(\vec{r})|^2 q$$

$$= |(\vec{r})|^2 (1 + 2q)$$

then

$$|(\vec{r}) + \vec{r}|^{-3} = \frac{1}{|(\vec{r})|^3} (1 + 2q)^{-3/2} \tag{43}$$

let

$$\left. \begin{array}{l} h = \dfrac{k^2 m_2}{r^3} \\[3mm] (h) = \dfrac{k^2 M}{|(\vec{r})|^3} \end{array} \right\} \tag{44}$$

Substituting equations (43) and (44) into (40) yields

$$\frac{d^2\vec{r}}{dt^2} = -h\vec{r} - k^2 M \left\{ ((\vec{r}) + \vec{r}) \frac{1}{|(\vec{r})|^3} (1 + 2q)^{-3/2} - \frac{(\vec{r})}{|(\vec{r})|^3} \right\}$$

$$= -h\vec{r} - (h) [(\vec{r}) + \vec{r}] (1 + 2q)^{-3/2} + (h)(\vec{r})$$

$$\frac{d^2\vec{r}}{dt^2} = [-h - (h)(1 + 2q)^{-3/2}] \vec{r} + (h)(\vec{r})[-(1 + 2q)^{-3/2} + 1] \tag{45}$$

now making the same series expansion as before

$$1 - (1 + 2q)^{-3/2} = q\left(3 - \frac{15}{2}q + \frac{35}{2}q^2 + \cdots\right)$$

$$= fq$$

the equations of motion become

$$\frac{d^2\vec{r}}{dt^2} = \{-h - (h)\,[1 - fq]\}\,\vec{r} + (h)\,(\vec{r})\,fq$$

or

$$\frac{d^2\vec{r}}{dt^2} = \{(h)\,fq - (h) - h\}\,\vec{r} + (h)\,fq\,(\vec{r}) \tag{46}$$

where the term due solely to the central body is $h\vec{r}$ and the rest is due to the presence of the sun.

Combining the Equations of Motion

The equations of motion are now combined to include the perturbations due to the sun and those due to other bodies. Rewrite equation (46) in the following form

$$\frac{d^2\vec{r}}{dt^2} = -h\vec{r} + \phi \tag{47}$$

where ϕ is the acceleration due to the presence of the sun

$$\phi = \{(h)\,fq - (h)\}\,\vec{r} + (h)\,fq\,(\vec{r}) \tag{48}$$

and

$$h = \frac{k^2 m_4}{r^3}$$

where r is the distance from Jupiter to the probe.

To include other bodies we must add to equation (47) the acceleration expressed as $\vec{F}$ in equation (39)

$$\frac{d^2\vec{r}}{dt^2} = -h\vec{r} + \phi + \vec{F} \tag{49}$$

where

$$\vec{F} = \sum_i k^2 m_i \left(\frac{\vec{r}_i' - \vec{r}}{\rho_i^3} - \frac{\vec{r}_i'}{r_i'^3} \right)$$

and $\vec{r}$ is the vector from Jupiter to the probe and $\vec{r}'$ is from Jupiter to the disturbing body.

Equation (49) represents Cowell's equation of motion. When Encke's procedure is wanted the following is used:

$$\frac{d^2\delta\vec{r}}{dt^2} = \frac{k^2 M_{2\!\!\!|}}{r_0^3} \delta\vec{r} + \frac{k^2 m_{2\!\!\!|}}{r_0^3} fq\vec{r} + \vec{F} + \phi. \tag{50}$$

Care must be taken in interpreting equations (48), (49) and (50) since f and q have different meanings depending on whether or not Encke's method is used.

Integration of the Equations of Motion

The above equations of motion either (49) or (50) are integrated over the time spent in the sphere of influence by means of a numerical integration technique (reference 17). This technique is a fourth order predictor-corrector with automatic adjustment of the time step of integration.

The integration is started at the time of the probe's entrance to the sphere of influence and is terminated at exit from the sphere. This termination is accomplished by checking the probe's distance from Jupiter until this distance becomes equal to the radius of the sphere. The integration is then halted and the resulting trajectory is determined.

In the actual computer runs made, the use of the above Encke's equation (50) more than tripled the computer time when the moons of Jupiter were included as perturbing bodies. This increase in time was due in part to the greater number of calculations required and to the number of rectifications that occurred because of the inclusion of the moons. For this reason Cowell's method was used exclusively for the results included in this report. Encke's method was used as a check in only a few cases to insure that numerical accuracy was being retained.

THE GALILEAN SATELLITES OF JUPITER

On the night of January 7, 1610 Galileo Galilei turned his crude telescope toward Jupiter and noticed three small "stars" in the vicinity of and in a straight line with the planet. Repeated observations showed that these "stars" moved with respect to Jupiter and on January 13 he saw four "stars". Further observations proved to him that he had indeed discovered satellites of Jupiter (reference 18).

The German astronomer Marius later independently discovered the Galilean moons and gave them their names (reference 19) as follows:

I Io

II Europa

III Ganymede

IV Callisto

Table III is a compilation of the physical data of these satellites and is taken in part from reference 20.

When we consider that the planet Mercury has on the same scale a diameter of 0.38, compared to 0.394 for Ganymede, we see that these moons are by no means small.

These four satellites have been found to be subject to very strong mutual perturbations which cause librations in their orbits about Jupiter. Laplace first discovered a resonance relationship between satellites I, II and III which shows that their mean motions are approximately in the proportion of 4:2:1 or in terms of mean longitudes $L_1 - 3L_2 + 2L_3 = 180$ degrees (reference 21). If one

30

Table III

The Galilean Satellites: Astronomical and Physical Data

	I_0	Europa	Ganymede	Callisto
Mass (Earth = 1)	0.0121	0.0079	0.0261	0.0160
Mean Diameter (Earth = 1)	0.255	0.226	0.394	0.350
Mean Density (H_2O = 1)	4.03	3.78	2.35	2.06
Surface Gravity (Earth = 1)	0.19	0.16	0.17	0.13
Velocity of Escape (km/sec)	2.5	2.1	2.9	2.4
Period of Axial Rotation (Days)	1.77	3.55	7.15	16.69
Mean Distance from Planet (km)	421,400	670,500	1,069,500	1,881,200
Sidereal Period (Days)	1.769	3.551	7.155	16.689
Mean Orbital Velocity (km/sec)	17.37	13.77	10.90	8.22
Radius of Sphere of Influence (km)	7,200	9,600	24,800	36,100

of the satellites is disturbed, the motions of the other two adjust so that this relationship is satisfied. Therefore the three satellites cannot be in conjunction or opposition at the same time (reference 22).

Little can be found in the literature on an accurate theory of the motions of the four moons but accurate positions are obviously necessary if a realistic investigation into their effects on the flyby probe is to be made. The theory of the moons is quite complex and interest in the theory has only recently begun to bring about useful investigations.

Sampson in 1910 (references 23 and 24) and De Sitter in 1931 (reference 25) have developed detailed theories to describe the motions of the Galilean satellites. Sampson's work is perhaps the best known and includes a rather extensive set of tables which are used to determine the position of the moons and to predict such physical phenomena as occulations and eclipses. This work which has become known as Sampson's Tables represents a monumental and

complex task. Although difficult to use these tables give the times of phenomena to 0.000001 days and positions to $0°.000001$ (reference 26). Andoyer (reference 27) somewhat simplified the procedure by using only the main terms of Sampson's tables and even though this is less accurate, Andoyer's procedure has been adopted by the Nautical Almanac Office in their publication of the phenomena of the moons.

More recently Ferraz Mello (reference 28) has studied the planar motion of the Galilean satellites in rectangular coordinates. He shows that the higher order harmonics of Jupiter's gravitational potential and the relativity corrections are negligable. Marsden (reference 29) has studied the motion of the four moons using Von Ziepel's method to eliminate the short period terms and to reduce the number of degrees of freedom.

The method used in this report to obtain the positions is a more or less simplified version of Sampson's method. The model used is one of a slowly moving plane common to all four satellites with some plane perturbations. This model leads to uncertainties in position of

300;	6000;	6000;	25000	kilometers

respectively for satellites I, II, III and IV when compared with Sampson's Tables (reference 30). This method was received from Dr. Jean L. Sagnier in Paris, France who has spent much time investigating the theory of the moons of Jupiter.

A complete description of the information received from Dr. Sagnier appears in Appendix D and a complete and extensive discussion of Sampson's theory of the moons can be found in reference 23. The Tables in Appendix D are used to determine the positions of the moons which are in turn necessary to evaluate the disturbing acceleration in equation (39) above. This method of obtaining the positions of the moons has been programmed to generate an ephemeris of positions for each of the four moons. Such ephemerides do not seem to be easily available elsewhere.

A comparison was made with examples worked out by Sampson in reference 20. Table IV shows the results of this comparison for satellites I and III on two different dates. The longitude is measured from the mean equinox of 1900 along the mean ecliptic to the ascending node of Jupiter's orbital plane and thereafter along this plane. The magnitude of the radius vector to the satellite is the projection of the radius vector into Jupiter's equatorial plane; and the column labeled "tan latitude" is the tangent of the elevation of the radius vector to Jupiter's orbital plane.

Table IV

Comparison of Sagnier's Method and Sampson's Tables (Jovicentered)

Satellite I June 2.156 1909	Longitude	Radii (A. U.)	Tan Latitude
simplified method	$336°.07021$	0.0000281304	.018832
Sampson's tables	$336°.06863$	0.0000281296	.0191815
|difference|	$0°.00158$	8×10^{-10}	.0003
Satellite III April 3.841 1910			
simplified method	$9°.92885$	0.00714796	.045659
Sampson's tables	$9°.92550$	0.00714794	.045686
|difference|	$0°.00335$	2×10^{-8}	.000027

ENCOUNTER GEOMETRIES AND MISSIONS USED IN THE STUDY

Twenty different trajectories were studied to determine the effects of the Galilean moons. The launch date for injection into the transfer orbit from the Earth to Jupiter was March 8, 1972 which is one of the dates under consideration for a Galactic Jupiter Probe currently being planned by NASA (reference 31). Flight times of 450, 500, 550 and 600 days from the Earth were used along with several combinations of the encounter parameters B and Ψ. The first twelve cases included flight times of 450, 500 and 550 days. The magnitude of the miss vector was held constant at 1.25×10^6 km and the angle Ψ was varied from 0 to 360 degrees in steps of 90 degrees. The remaining 8 cases were obtained using a constant value of $180°$ for Ψ and values of 1.0×10^6 and 1.5×10^6 km for B. A flight time of 600 days was also included in these cases. These 8 cases represent the type of encounter geometry that is particularly useful in obtaining hyperbolic heliocentric trajectories which are capable of achieving far distances in relatively short times.

Some of the first twelve trajectories, particularly those where $\Psi = 0°$, are also useful for solar probes since they result in eccentricities of almost 1. These trajectories can in some cases impact the sun which cannot be done with direct flights from the Earth because of the energy required (references 8 and 11). However for these trajectories it is desirable that at exit from Jupiter's sphere of influence the probe be heading toward the sun, i.e. that the heliocentric true anomaly be greater than $180°$. Otherwise the time required for the probe to reach the sun is increased prohibitively.

Values of 90° and 270° for Ψ are very useful in obtaining large distances both above and below the ecliptic plane and a little reflection will reveal that the two values ought to give symmetrical results (reference 8). Indeed it is possible to obtain a distance of 30 a.u. out of the ecliptic as did the case for 450 days where $\Psi = 270°$. However the time required to reach such distances will also be considerable and may rule out the possibility of such a flight being undertaken.

Other types of missions may also be studied if desired. These could include obtaining high inclinations of the orbit plane with the ecliptic, maximum velocity normal to the ecliptic and many other interesting orbits. Most of these would be difficult to attain in terms of the energy requirements without using the gravitational attraction of a large planet. This report includes only three types of mission objectives: the time required to reach 10 a.u. from the sun, the maximum distance attained out of the ecliptic, and close approaches to or impact with the sun.

RESULTS AND CONCLUSIONS

The effects of the Galilean moons of Jupiter on the Jovian centered orbit are presented in Table V. These results are presented as differences resulting from using only the sun as a disturbing body and then using the sun and moons as disturbing bodies. The first three columns identify the case with the parameters B in kilometers, Ψ in degrees and transfer time in days. The next six columns are the differences in the Keplerian elements as follows: the semi major axis (a), eccentricity (e), inclination (i), true anomaly (θ), right ascension of the ascending node (Ω), and arguement of perojove (ω). The next column is the difference in magnitude of the velocity at exit from Jupiter's sphere of influence. As described in a previous section the integration of the equations of motion is terminated when the probe reaches a distance of 48×10^6 kilometers from Jupiter which is the radius of the sphere of influence. Therefore, the magnitude of the radius vector is always the same at exit and differences can occur only in tangential position and in the velocity vector. The final four columns show the closest approach to the Galilean moons. The closest approaches to all four moons always occur within a span of 1.5 days and always near perijove of the approach trajectory where the probe is moving very fast.

A quick glance at the $\triangle$ a column shows that the only large differences occur in cases 11 and 19. The semi major axis is computed from

$$a = \frac{r}{2 - \dfrac{r v^2}{\mu}}$$

36

and since r is constant, the change in a is dependent only on v. Case 11 passes Europa by 6100 km and is the closest approach of all the cases. A close approach to one or more of the moons will of course perturb the trajectory. A study was made for case 11 in which one moon at a time was included into the equations of motion. Europa by itself caused about half of the perturbation and inclusion of Ganymede accounted for almost all of the remaining perturbation. However, Ganymede by itself accounted for little of the total perturbation. Hand calculations independent of the program substantiated the results obtained when a single moon was included. This study shows that a complex dynamical inter- action between the bodies is occurring. This complex interaction cannot be predicted analytically in an easy way and therefore the perturbation is difficult to prove conclusively.

The change occurring in case 19 is even more difficult to explain. This trajectory does come closer to Ganymede than any other trajectory but is well outside Ganymede's sphere of influence (see table III). This case represents a 600 day transfer trajectory and as such is a relatively low energy Jupiter centered trajectory. Because of its low energy it is more sensitive to perturb- ing forces. As in case 11 approximate methods tended only to confirm the re- sults obtained using one moon at a time. Again the explanation lies in the dynamical interaction between the bodies.

The other 18 cases do not exhibit any abnormally large changes in any of the elements.

It therefore appears from Table V that the moons of Jupiter do not repre- sent any major perturbative force as far as the Jovian centered trajectory is concerned in a majority of the cases. This is consistent with what was originally thought when the problem was first undertaken. However, cases 11 and 19 indicate that under the right dynamical conditions, significant perturbations may result that will have to be considered. These perturbations cannot be predicted without including the moons.

Table VI shows the resulting effects of the moons on the heliocentric trajectories at post encounter. The columns are the same as for Table V except a column has been added for the difference in the heliocentric radial distances.

Large differences occur in the semi major axis for the heliocentric orbits, which by virtue of the above equation are attributed to changes in the position and velocity magnitudes. Although these are large variations, it must be pointed out that the semi major axis is itself large. For example Case 12 shows a change in a of $.12 \times 10^9$ km, where a equals 3×10^9 km, representing a perturbation of about 4%. This is the largest percentage of all 20 cases.

Cases 11 and 19 in the heliocentric orbits do not exhibit the large perturbations that occurred in the Jovicentric orbits. The variations in the semi major axis in the heliocentric cases are much less than 1%. Indeed a glance at Table VI shows that none of the elements change very much and some exhibit smaller changes than the other 18 cases.

Table VII shows the differences resulting in the parameters that are of interest for a deep space post Jupiter encounter mission. The first three columns are the same as the previous tables. Columns 4 and 5 are found by taking the square root of the sum of the squares of the differences in components of the Jovicentric position and velocity vectors respectively. These numbers represent the straight line distance and velocity between the two types of perturbation runs. Column 6 is the difference in the time spent in Jupiter's sphere of influence. Columns 7, 8 and 9 are the respective differences in time to reach 10 a.u. from the sun; distances attained out of the ecliptic; and closest approach to the sun where these missions are applicable. Again the last 4 columns are a repetition of the close approaches to the moons.

Figure 10 (from reference 9) is a contour map of constant times to 10 A.U. This map was done for a 500 day transfer time and is in the $\vec{T}$ and $\vec{R}$ plane

which is defined in a previous section. This plane is commonly called the impact plane and is perpendicular to the incoming asymptote. The angle Ψ is measured around the perimeter of the figure and the magnitude of the miss vector (B) is measured by the concentric circles. A flight time of 600 days from post encounter to 10 A.U. can be achieved by any combination of the parameters B and Ψ as obtained from the 600 day contour line. Anything inside this line represents a flight time of less than 600 days. The launch date for this figure was March 10, 1972 which is two days later than the launch date for Case 7 in Table V, but this difference will not alter Figure 10 by any appreciable amount. Figure 10 was drawn using only a two body determination as outlined in a previous section. Case 7 in Table VII took 558.990 days to reach 10 A. U. when the sun and moons were included as perturbing bodies. The undisturbed time in Figure 10 was 556.528 days. From Table VII the time difference caused by the moons of Jupiter was 0.12 days. Cases 3 and 4 in Table VI may also be located on this contour map for B equal to 1.0×10^6 and 1.5×10^6 km respectively. Again it is seen that the influence of the moons is negligible. Also the difference between the perturbed and two body determination used in Figure 10 was less than four days so even the sun makes only a small difference as a disturbing body.

As far as the mission is concerned it is seen that the effects of the moons are very small indeed and can be neglected. However as far as determining the precise point of exit from the sphere of influence, columns 4 and 5 of Table VII clearly indicate that the moons do have an effect. These effects could be of critical importance depending on the particular post encounter mission being contemplated. This along with the changes in the heliocentric semi-major axis is sufficient to conclude that for purposes of orbit determination the Galilean moons must be included in any realistic study of a Jupiter Flyby.

Table V

Effects of the Galilean Moons on the Jovicentric Orbital Elements

B (km)	ψ (deg.)	Flight Time (Days)	Δa (km)	Δe	Δi (deg.)	Δω (deg.)	ΔΩ (deg.)	Δα (deg.)	Δv (km/sec)	Io (km)	Europa (km)	Ganymede (km)	Callisto (km)
1.25×10^6	0	450	90	0.0094	0	0.13	0.03	0.03	0.001	534,000	140,000	156,000	547,000
1.25×10^6	90	450	20	0.0017	0.188	0.02	0.134	0.03	0	622,000	815,000	1,270,000	1,140,000
1.25×10^6	180	450	30	0.0055	0.006	0.07	0.0280	0.11	0	453,000	1,130,000	1,710,000	1,510,000
1.25×10^6	270	450	20	0.0026	0.227	0.03	0.04	0.04	0	582,000	754,000	1,290,000	1,280,000
1.25×10^6	0	500	40	0.0049	0	0.10	0.04	0.03	0.001	464,000	71,100	232,000	88,800
1.25×10^6	90	500	50	0.0036	0.094	0.08	0.04	0.10	0.001	489,000	447,000	1,360,000	1,350,000
1.25×10^6	180	500	100	0.0022	0.008	0.04	0.0344	0.18	0.001	356,000	673,000	1,820,000	1,870,000
1.25×10^6	270	500	40	0.0042	0.041	0.09	0.10	0.09	0.001	471,000	380,000	1,340,000	1,440,000
1.25×10^6	0	550	600	0.0053	0.01	0.18	0.03	0.28	0.003	338,000	139,000	543,000	435,000
1.25×10^6	90	550	400	0.0010	0.388	0.04	0.19	0.01	0.001	801,000	332,000	1,200,000	1,630,000
1.25×10^6	180	550	6,200	0.0034	0.225	0.12	0.377	0.47	0.030	806,000	6,140	1,490,000	2,230,000
1.25×10^6	270	550	400	0.0007	0.417	0.02	0.13	0.01	0.002	823,000	358,000	1,160,000	1,680,000
1.0×10^6	180	450	4	0.0049	0.004	0.08	0.0275	0.15	0	199,000	787,000	1,530,000	1,310,000
1.5×10^6	180	450	20	0.0072	0.006	0.06	0.0280	0.08	0.001	716,000	1,430,000	1,890,000	1,700,000
1.0×10^6	180	500	140	0.0026	0.008	0.08	0.0346	0.24	0.001	345,000	255,000	1,610,000	1,690,000
1.5×10^6	180	500	150	0.0008	0.006	0.01	0.0303	0.11	0.001	561,000	1,020,000	2,030,000	2,060,000
1.0×10^6	180	550	500	0.0051	0.001	0.25	0.0268	0.25	0.003	794,000	98,800	1,070,000	2,060,000
1.5×10^6	180	550	300	0.0077	0.007	0.20	0.0131	0.16	0.001	672,000	274,000	1,810,000	2,390,000
1.0×10^6	180	600	4,100	0.0068	0.057	0.47	0.0175	0.13	0.0127	619,000	764,000	140,000	2,170,000
1.5×10^6	180	600	200	0.0057	0.014	0.23	0.0198	0.04	0.0005	1,190,000	803,000	933,000	2,630,000

Table VI

Effects of the Galilean Moons on the Heliocentric Orbital Elements

B (km)	ψ (deg.)	Flight Time (Days)	Δa (km)	Δe	Δi (deg.)	$\Delta \theta$ (deg.)	$\Delta \Omega$ (deg.)	$\Delta \omega$ (deg.)	ΔR (km)*	Δv (km/sec)	IO (km)	Europa (km)	Ganymede (km)	Callisto (km)
1.25×10^6	0	450	310,000	.0001	0.01	0	0.56	0.52	100,000	0.0270	534,000	140,000	156,000	547,000
1.25×10^6	90	450	713,000	.00331	0.086	0.135	0.081	0.20	50,000	0.024	622,000	815,000	1,270,000	1,140,000
1.25×10^6	180	450	2,510,000	.0056	0.001	0.148	0.0039	0.16	40,000	0.020	453,000	1,130,000	1,710,000	1,510,000
1.25×10^6	270	450	104,700,000	.00356	0.089	0.141	0.04	0.12	40,000	0.024	582,000	754,000	1,290,000	1,280,000
1.25×10^6	0	500	540,000	0	0.175	0	0.73	0.22	80,000	0.189	464,000	71,100	232,000	88,800
1.25×10^6	90	500	15,400,000	.00229	0.045	0.005	0.05	0.05	50,000	0.013	489,000	447,000	1,360,000	1,350,000
1.25×10^6	180	500	2,090,000	.0034	0.003	0.090	0.0083	0.11	40,000	0.013	356,000	673,000	1,820,000	1,870,000
1.25×10^6	270	500	23,700,000	.00262	0.048	0.029	0.02	0.03	40,000	0.014	471,000	380,000	1,340,000	1,440,000
1.25×10^6	0	550	1,730,000	.00125	0.046	0.021	0.1554	0.33	370,000	0.0929	338,000	139,000	543,000	435,000
1.25×10^6	90	550	73,500,000	.00965	0.121	0.279	0.189	0.10	240,000	0.046	801,000	332,000	1,200,000	1,630,000
1.25×10^6	180	550	6,530,000	.0062	0.053	0.012	0.1800	0.19	0	0.027	806,000	6,140	1,490,000	2,230,000
1.25×10^6	270	550	119,800,000	.0101	0.143	0.290	0.07	0.32	230,000	0.047	823,000	358,000	1,160,000	1,680,000
1.0×10^6	180	450	2,030,000	.0081	0.001	0.182	0.0049	0.20	90,000	0.026	199,000	787,000	1,530,000	1,310,000
1.5×10^6	180	450	2,990,000	.0040	0.001	0.127	0.0032	0.13	30,000	0.016	716,000	1,430,000	1,890,000	1,700,000
1.0×10^6	180	500	1,470,000	.0041	0.003	0.101	0.0099	0.11	70,000	0.014	345,000	255,000	1,610,000	1,690,000
1.5×10^6	180	500	3,000,000	.0026	0.002	0.079	0.0068	0.09	20,000	0.011	561,000	1,020,000	2,030,000	2,060,000
1.0×10^6	180	550	5,220,000	.0096	0	0.312	0.0022	0.68	300,000	0.036	794,000	98,800	1,070,000	2,060,000
1.5×10^6	180	550	13,600,000	.0087	0.001	0.286	0.0036	0.30	140,000	0.036	672,000	274,000	1,810,000	2,390,000
1.0×10^6	180	600	480,000	.0009	0.005	0.191	0.0148	0.19	230,000	0.004	619,000	764,000	140,000	2,170,000
1.5×10^6	180	600	10,700,000	.0047	0	0.179	0	0.19	130,000	0.020	1,190,000	803,000	933,000	2,630,000

This column is the differences in heliocentric radial distances and not rss values.

Table VII

Effects of the Galilean Moons on Deep Space Mission Parameters

B (km)	ψ (deg.)	Flight Time (Days)	Total Position Deviation at Exit From Sphere (km)*	Total Velocity Deviation at Exit From Sphere (km/sec)*	Time in Sphere (Days)	Time to 10 A.U. (Days)	Dist. out of Ecliptic A.U.	Closest Approach to Sun (km)	Io (km)	Europa (km)	Ganymede (km)	Callisto (km)
1.25×10^6	0	450	107,000	0.0317	0.001	—	—	—	534,000	140,000	156,000	547,000
1.25×10^6	90	450	110,000	0.0358	0.002	2.84	0.590 0.008	—	622,000	815,000	1,270,000	1,140,000
1.25×10^6	180	450	122,000	0.0375	0.006	0.18	—	—	453,000	1,130,000	1,710,000	1,510,000
1.25×10^6	270	450	110,000	0.0356	0.002	2.75	0.827 0.010	—	582,000	754,000	1,290,000	1,280,000
1.25×10^6	0	500	76,400	0.0194	0.004	—	—	Impact	464,000	71,100	232,000	88,800
1.25×10^6	90	500	82,200	0.0248	0.006	3.4	0.083 0.006	—	489,000	447,000	1,360,000	1,350,000
1.25×10^6	180	500	84,100	0.0226	0.008	0.12	—	—	356,000	673,000	1,820,000	1,870,000
1.25×10^6	270	500	82,100	0.0217	0.006	3.28	0.110 0.006	—	471,000	380,000	1,340,000	1,440,000
1.25×10^6	0	550	416,800	0.0938	0.020	—	—	656,000	338,000	139,000	543,000	435,000
1.25×10^6	90	550	352,800	0.0814	0.006	16.5	0.201 0.010	—	801,000	332,000	1,200,000	1,630,000
1.25×10^6	180	550	146,800	0.0448	0.133	1.49	—	—	806,000	6,140	1,490,000	2,230,000
1.25×10^6	270	550	356,200	0.0821	0.006	14.9	0.002 0.029	—	823,000	358,000	1,160,000	1,680,000
1.0×10^6	180	450	176,800	0.0546	0.004	0.06	—	—	199,000	787,000	1,530,000	1,310,000
1.5×10^6	180	450	92,000	0.0276	0.005	0.21	—	—	716,000	1,430,000	1,890,000	1,700,000
1.0×10^6	180	500	110,000	0.0301	0.005	0	—	—	345,000	255,000	1,610,000	1,690,000
1.5×10^6	180	500	64,400	0.0173	0.009	0.19	—	—	561,000	1,020,000	2,030,000	2,060,000
1.0×10^6	180	550	398,000	0.0895	0.022	1.28	—	—	794,000	98,800	1,070,000	2,060,000
1.5×10^6	180	550	288,700	0.0643	0.012	0.53	—	—	672,000	274,000	1,810,000	2,390,000
1.0×10^6	180	600	288,000	0.0526	0.050	1.11	—	—	619,000	764,000	140,000	2,170,000
1.5×10^6	180	600	210,300	0.0400	0.010	0.21	—	—	1,190,000	803,000	933,000	2,630,000

* These deviations are Jovicentric and are the square root of the sum of the squares of the component deviations
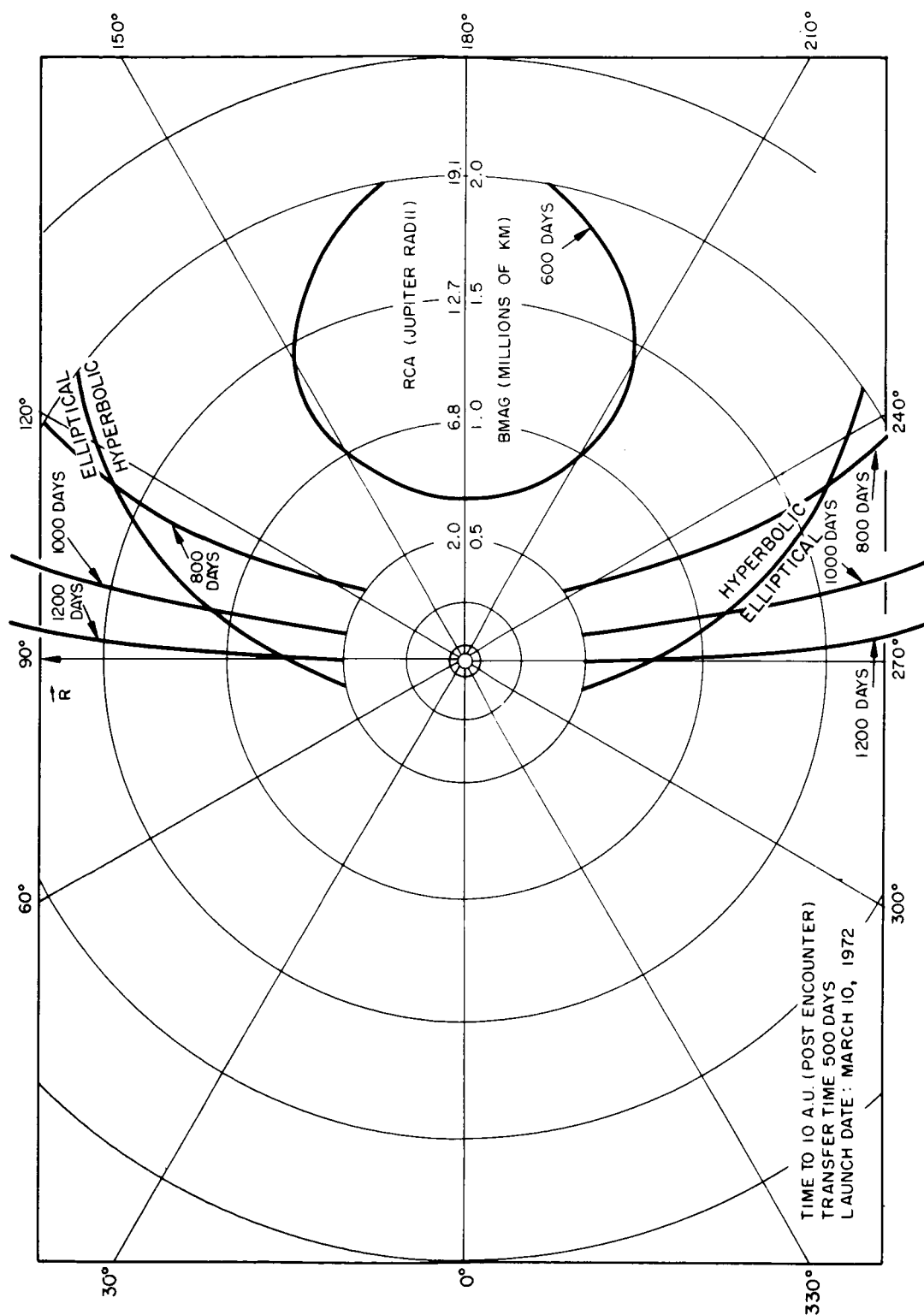
Figure 10—Constant Contours of Time to 10 A.U. (From Reference 9)

SUMMARY

The effects of the Galilean moons of Jupiter on a probe passing close to Jupiter were studied by using two different perturbative schemes. The first included only the sun as a perturbing body and the second included the sun and the four moons. Variations obtained from the two models are then the effects of the presence of the moons. An integrated trajectory was used only within Jupiter's sphere of influence with an approximate two body determination of the transfer trajectory between the Earth and Jupiter.

The numerical integration method was a predictor-corrector scheme with automatic adjustment of the step size and automatic error control. Due to considerable savings in machine time all cases were studied by integrating Cowell's equations of motion rather than Encke's equations.

While the total variations due to the Galilean moons in the Jovian centered orbital elements of the probe during the Jupiter flyby are fairly small, the actual point of exit on the sphere of influence is changed by an appreciable amount. Therefore as concerning gross trajectory determination one can essentially neglect these moons but when accurate position and velocity vectors are required, the perturbative effects of the moons most certainly should be included.

It is shown that the post encounter mission objectives such as time to reach 10 a.u. from the sun are also little changed due to the presence of the four larger moons of Jupiter. However the semi-major axis of the resulting heliocentric orbits do undergo large variations. The importance of the perturbations will

depend on the exact nature of the post encounter missions that are to be studied such as a close approach to a second outer planet. Thus for accurate trajectory determination as well as accurate positions and velocities it is advisable to include the Galilean moons in the equations of motion.

APPENDIX A

TO COMPUTE TIME FROM PERIAPSIS TO A GIVEN TRUE ANOMALY

This problem is easily solved using two body equations and the solution of Kepler's equation yields the desired result immediately.

Let: a be the semi-major axis

    e the eccentricity

    θ the true anomaly

    n the mean motion

    ρ the semi latus rectum

    t the time from periapsis

    m the mean anomaly

    E the eccentric anomaly

    r magnitude of radius vector

The relationship between θ and E can be seen from figure A-1.

Now
$$X = \xi - ae = a\,(\cos E - e) = r\,\cos\theta \qquad\qquad \text{(A-1)}$$

$$Y = \eta = b\,\sin E = r\,\sin\theta \qquad\qquad \text{(A-2)}$$

$$b = a\,\sqrt{1 - e^2}$$

also

$$r = \frac{a\,(1 - e^2)}{1 + e\,\cos\theta} \qquad\qquad \text{(A-3)}$$

from (A-1) and (A-2) we obtain

$$r = a\,(1 - e\,\cos E) \qquad\qquad \text{(A-4)}$$

46

from (A-1), (A-2), and (A-4), we obtain

$$\cos \theta = \frac{\cos E - e}{1 - e \cos E}$$

$$\sin \theta = \frac{\sqrt{1 - e^2} \sin E}{1 - e \cos E}$$

and this allows us to finally obtain

$$\text{Tan} \frac{E}{2} = \sqrt{\frac{1 - e}{1 + e}} \; \text{Tan} \; \frac{\theta}{2} \tag{A-5}$$

The mean motion n is defined to be

$$n = \sqrt{\frac{\mu}{a^3}}$$

where μ is the gravitational constant of the central body. Using (A-5) to obtain E , Kepler's equation states that for an ellipse

$$M = E - e \sin E = nt \tag{A-6}$$

Therefore

$$t = \frac{M}{n} \tag{A-7}$$

For an hyperbola, Kepler's equation becomes

$$M = e \sinh E - E \tag{A-8}$$

and again equation (A-7) holds.

For a parabola, a slightly different treatment is necessary. Equation (A-3) may be written as follows:

$$r = \frac{a (1 - e) (1 + e)}{1 + e \cos \theta}$$

let $q = a (1 - e)$

then upon setting $e = 1$

$$r = \frac{2q}{1 + \cos \theta} \tag{A-9}$$

Define

$$D = \sqrt{2q} \; \text{t an} \frac{\theta}{2}$$

then

$$r = \frac{1}{2} (2q + D^2) \tag{A-10}$$

The area using equation (A-10) is

$$A = \frac{1}{2} \int_0^{\theta} r^2 \, d\theta$$

$$= \frac{1}{2} \sqrt{2q} \left(qD + \frac{D^3}{6} \right)$$

This yields

$$t = \frac{1}{\sqrt{\mu}} \left(qD + \frac{D^3}{6} \right) \tag{A-11}$$

where

$$n = \sqrt{\mu}$$

equation (A-11) may be found developed fully in reference 3. Equations (A-5), (A-6), (A-7), and (A-11) then allows one to compute the time for any type of orbit.
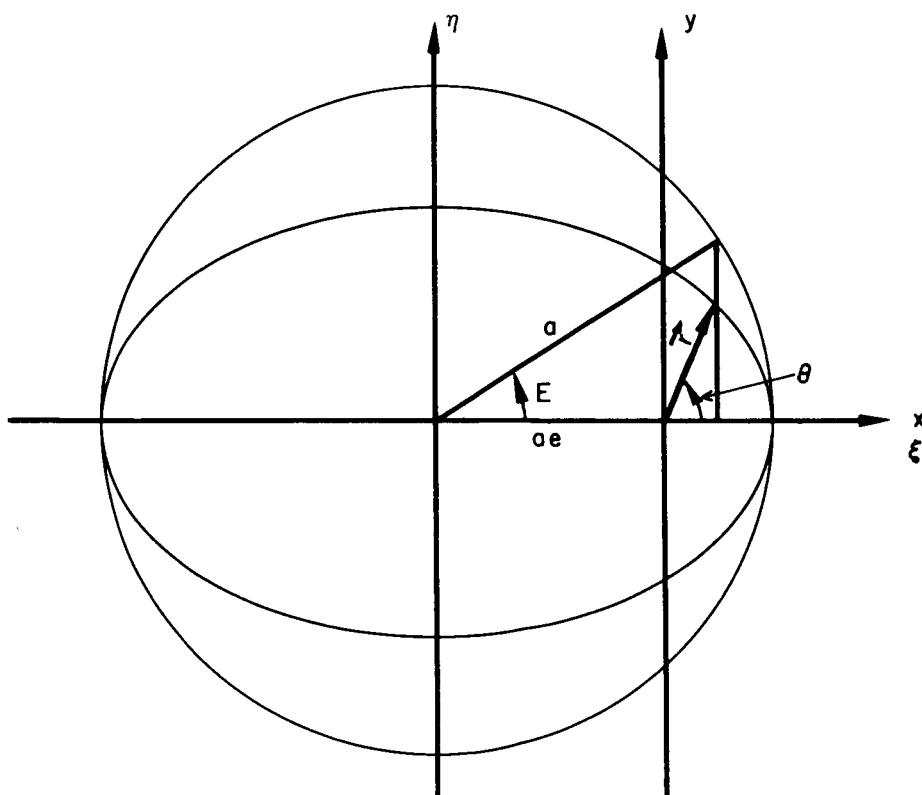
Figure A-1—Relationship Between True Anomaly and
Eccentric Anomaly

APPENDIX B

TO UPDATE THE CARTESIAN COORDINATES OF THE PROBE
USING AN INCREMENTAL TRUE ANOMALY

The problem to be solved here is that of determining the position and velocity of a probe which is separated from a known position and velocity by an increment in the true anomaly. This treatment is essentially that found in reference 7. The following notation will be used:

μ gravitational constant of the central body

$\vec{r}_0$ initial position

$\vec{v}_0$ initial velocity

$\vec{H} = \vec{r}_0 \times \vec{v}_0$ momentum vector

$h = |\vec{H}|$

$\delta = \theta - \theta_0$ the incremental true anomaly

$\vec{r}$ final position

$\vec{v}$ final velocity

Since we are considering only two body planer motion we may write the following relationships:

$$\left.\begin{array}{l} \vec{r} = f\,\vec{r}_0 + g\vec{v}_0 \\[2mm] \vec{v} = \dot{f}\,\vec{r}_0 + \dot{g}\,\vec{v}_0 \end{array}\right\} \tag{B-1}$$

The quantities we wish to find are f, g, $\dot{f}$, and $\dot{g}$.

49
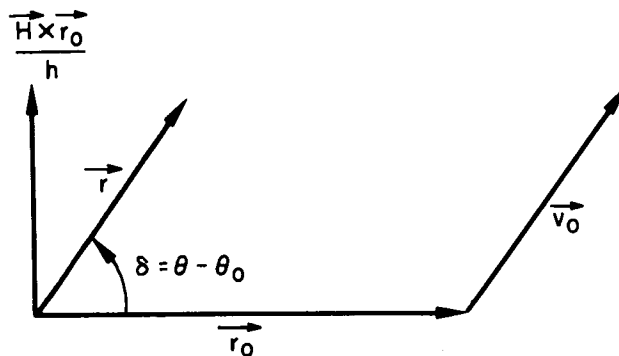
Figure B-1—Updating the Cartesian Coordinates

Figure B-1 will be helpful in understanding the geometry of the problem. We first compute the momentum vector

$$\vec{H} = \vec{r}_0 \times \vec{v}_0$$

and observe that

$$\frac{\vec{H} \times \vec{r}_0}{h}$$

has magnitude equal to r_0.

From figure B-1 we can decompose $\vec{r}$ onto $\vec{r}_0$ and $\dfrac{\vec{H}_0 \times \vec{r}_0}{h}$ and obtain respectively $r \cos \delta$ and $r \sin \delta$.

We may therefore write for $\vec{r}$

$$\vec{r} = \frac{r}{r_0} \left[\vec{r}_0 \cos \delta + \frac{\vec{H} \times \vec{r}_0}{h} \sin \delta \right] \tag{B-2}$$

and

$$\vec{H} \times \vec{r}_0 = (\vec{r}_0 \times \vec{v}_0) \times \vec{r}_0 = \vec{v}_0 (\vec{r}_0 \cdot \vec{r}_0) - \vec{r}_0 (\vec{r}_0 \cdot \vec{v}_0)$$

then equation (B-2) becomes

$$\vec{r} = \frac{r}{r_0} \left[\vec{r}_0 \left(\cos \delta - \frac{\vec{r}_0 \cdot \vec{v}_0}{h} \sin \delta \right) + \vec{v}_0 \frac{r_0^2}{h} \sin \delta \right] \tag{B-3}$$

Comparing this with equation (B-1), we see that

$$f = \frac{r}{r_0} \left(\cos \delta - \frac{\vec{r}_0 \cdot \vec{v}_0}{h} \sin \delta \right)$$

$$g = \frac{r \, r_0}{h} \sin \delta$$

$$\left. \right\} \qquad \text{(B-4)}$$

However, the magnitude r in the above equation is still unknown. To solve for r we make use of the radius equation

$$r = \frac{a(1 - e^2)}{1 + e \cos \theta} = \frac{\rho}{1 + e \cos \theta}$$

and

$$a(1 - e^2) = \frac{h^2}{\mu}$$

Thus

$$r = \frac{h^2}{\mu(1 + e \cos \theta)} \qquad \text{(B-5)}$$

also

$$\theta = \delta + \theta_0$$

Therefore

$$\cos \theta = \cos \delta \cos \theta_0 - \sin \delta \sin \theta_0 \qquad \text{(B-6)}$$

Using equations (B-5) and (B-6), we immediately obtain

$$\cos \theta_0 = \frac{h^2 - \mu r_0}{\mu r_0 e} \qquad \text{(B-7)}$$

Note that from the radius equation we may write

$$\dot{r}_0 = \frac{d}{dt} (\vec{r}_0 \cdot \vec{r}_0)^{1/2} = \frac{\vec{r}_0 \cdot \vec{v}_0}{r_0}$$

$$= \frac{e \rho \dot{\theta} \sin \theta_0}{(1 + e \cos \theta_0)^2}$$

and by using

$$h = r_0^2 \, \dot{\theta}_0$$

we obtain

$$\sin \theta_0 = \frac{h \, \dot{r}_0}{\mu e} \tag{B-8}$$

from above

$$\dot{r}_0 = \frac{\vec{r}_0 \cdot \vec{v}_0}{r_0} \tag{B-9}$$

which together with equation (B-8) gives

$$\sin \theta_0 = \frac{h \, \vec{r}_0 \cdot \vec{v}_0}{r_0 \, \mu e} \tag{B-10}$$

using equations (B-5), (B-6), (B-7), and (B-10) we obtain

$$r = \frac{\frac{h^2}{\mu}}{1 + e \left[\frac{\cos \delta \, (h^2 - \mu r_0)}{\mu r_0 e} - \sin \delta \sin \theta_0 \right]}$$

or

$$\frac{r}{r_0} = \frac{h^2}{\mu r_0 + (h^2 - \mu r_0) \cos \delta - h \, (\vec{r}_0 \cdot \vec{v}_0) \sin \delta} \tag{B-11}$$

Equation (B-11) allows the computation of f and g in equation (B-4) above. In an entirely similar manner we may also obtain $\dot{f}$ and $\dot{g}$:

$$\left. \begin{aligned} \dot{f} &= \frac{\mu}{r_0 h^2} \left[(\vec{r}_0 \cdot \vec{v}_0) \, (1 - \cos \delta) - h \sin \delta \right] \\ \dot{g} &= 1 - \frac{\mu r_0}{h} (1 - \cos \delta) \end{aligned} \right\} \tag{B-12}$$

We may gain as a dividend the time difference corresponding to δ in the following manner:

$$a = \frac{r_0}{\left(2 - \frac{r_0 v^2}{\mu} \right)}$$

$$\rho = \frac{h^2}{\mu} = a(1 - e^2)$$

which yields

$$e^2 = 1 - \frac{\rho}{a}$$

From equations (B-7) and B-10) for θ we obtain

$$\text{Tan } \theta = \frac{h(\vec{r} \cdot \vec{v})}{h^2 - \mu r}$$

then

$$\theta = \theta_0 + \delta$$

and the method of Appendix A will yield the time difference between θ_0 and θ.

TO FIND $\vec{r}$ AND $\vec{v}$ OF A PROBE ON AN HYPERBOLIC
ORBIT SEPARATED FROM $\vec{r}_0$ AND $\vec{v}_0$ BY TIME Δt

The following method is used to step along an hyperbolic orbit knowing an initial position and velocity $\vec{r}_0$ and $\vec{v}_0$ and a time difference Δt.

Reference to figure C-1 shows the hyperbola and the geometry of the problem to be solved. The axis $\vec{i}_\xi$ and $\vec{i}_\eta$ are unit vectors, origin at the focus and such that they form a right handed system.
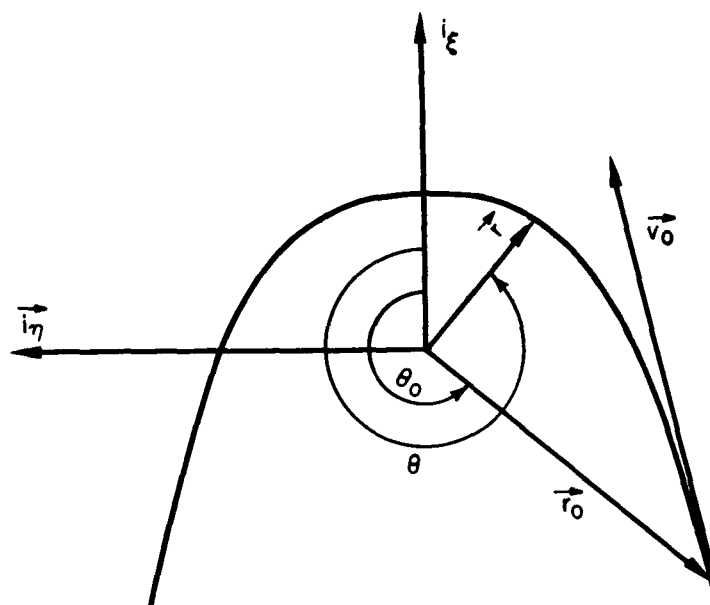
Figure C-1—The Hyperbolic Orbit Geometry

From figure C-1 it is obvious that

$$\vec{r} = r \cos \theta \, \vec{i}_{\xi} + r \sin \theta \, \vec{i}_{\eta} \tag{C-1}$$

and the well known relationships for a hyperbola are:

$$r = a \, (e \cosh F - 1) \tag{C-2}$$

$$\cos \theta = \frac{e - \cosh F}{e \cosh F - 1} \tag{C-3}$$

$$\sin \theta = \frac{\sqrt{e^2 - 1} \, \sinh F}{e \cosh F - 1} \tag{C-4}$$

where F is the "hyperbolic" eccentric anomaly. Upon substituting (C-2), (C-3), and (C-4) into (C-1), we obtain

$$\vec{r} = a(e - \cosh F) \, \vec{i}_{\xi} + \sqrt{a\rho} \, \sinh F \, \vec{i}_{\eta} \tag{C-5}$$

where ρ is the semi latus rectum. Differentiating equation (C-5) and noting that from Kepler's equation

$$\frac{dF}{dt} = \sqrt{\frac{\mu}{a^3}} \, \frac{1}{e \cosh H - 1}$$

we obtain

$$\vec{v} = -\frac{\sqrt{\mu a}}{r} \sinh F \, \vec{i}_{\xi} + \frac{\sqrt{\mu\rho}}{r} \cosh F \, \vec{i}_{\eta} \tag{C-6}$$

Equations (C-5) and (C-6) allow the computation of position and velocity anywhere along the hyperbola if the parameter F is known since a, e, and ρ may be easily calculated from $\vec{r}_0$ and $\vec{v}_0$. We will use $\vec{r}_0$ and $\vec{v}_0$ to calculate F and to determine the axis $\vec{i}_{\xi}$ and $\vec{i}_{\eta}$.

From the Laplace Integral of two body motion we have

$$\vec{E} = \frac{1}{\mu} \vec{v}_0 \times \vec{c}_0 - \vec{r}^{\,\circ}_0 \tag{C-7}$$

where $\vec{E}$ is a vector in the direction of perihelion and

$$\vec{c}_0 = \vec{r}_0 \times \vec{v}_0$$

Obviously

$$\vec{i}_{\xi} = \frac{\vec{E}}{|\vec{E}|} \tag{C-8}$$

also

$$\vec{i}_{\eta} = \frac{\vec{c}_0 \times \vec{E}}{|\vec{c}_0| \, |\vec{E}|} \tag{C-9}$$

From the energy equation we have

$$a = \frac{\mu r_0}{2\mu - r_0 v_0^2}$$

then

$$\rho = a \, |(e^2 - 1)|$$

where

$$e = |\vec{E}|$$

The mean motion is then

$$n = \sqrt{\frac{\mu}{a^3}}$$

and the true anomaly at the initial time is

$$\theta_0 = \cos^{-1} \left(\frac{\rho - r_0}{r_0 e} \right)$$

The change in the "hyperbolic" mean anomaly is

$$\Delta M = n \Delta t \tag{C-10}$$

The value for F_0 the eccentric anomaly at the initial point is obtained from

$$\sinh F_0 = \frac{\sqrt{e^2 - 1} \sin \theta_0}{e \cos \theta_0 + 1}$$

Then the value of the mean anomaly (M) at the point $\vec{r}$ is obtained by adding equation (C-10) to Kepler's equation evaluated at F_0

$$M = e \sinh F_0 - F_0 + \Delta M$$

or

$$M = e \sinh F - F \tag{C-11}$$

where F is the unknown eccentric anomaly needed in equations (C-5) and (C-6). Equation (C-11) can be solved for F by an interative procedure as follows:

we form the difference function

$$\triangle_n = M - e \sinh F_n + F_n \qquad \text{(C-12)}$$

and as a first guess we choose $F_1 = 0$. Using the Newton interative formula we have

$$F_{n+1} = F_n - \frac{\triangle_n}{\triangle'_n}$$

or

$$F_{n+1} = F_n - \frac{(M - e \sinh F_n + F_n)}{1 - e \cosh F_n} \qquad \text{(C-13)}$$

when $\triangle_n$ becomes small enough we have the required value for F and $\vec{r}$ and $\vec{v}$ may now be evaluated.

APPENDIX D

Received from Dr. J. L. Sagnier, Paris, France

THE POSITIONS OF JUPITER'S GREAT SATELLITES

The following tables include:

- The initial values and daily motions of the arguments occurring in the subsequent series, expressed in radians when taking into account the factor 2π.

- The series defining the mean positions of Jupiter's equatorial plane and of the orbital planes of the satellites.

- The equatorial true longitudes of the satellites, in radians from Sampson's x-axis up to the ascending node of Jupiter's equator on Sampson's (x, y)-plane, and thereafter along Jupiter's equator.

- The projected values on Jupiter's equator of the radii vectors, expressed in A. U.

- The reductions to Sampson's (x, y)-plane, to be added to the equatorial true longitudes, when the longitudes in Sampson's system are needed.

- The tangents of the latitudes on Sampson's (x, y)-plane.

The unit of time is always the ephemeris day, initial epochs are explicitly given when necessary. The unit of angle is the radian, except for some phase angles in the arguments expressed in degrees. The unit of length is the astronomical unit.

A low accuracy determination of the positions of Jupiter's satellites may be conveniently obtained by the introduction of the most significant terms of the radii vectors and of the equatorial longitudes in the mean orbital planes, whether approximated by the Jovian equator or not. But the use of the series reducing longitudes to Sampson's system and of those giving the latitudes in the same, is necessary for a full accuracy computation.

Arguments of Series

Arg^t	Value for 0^h TE, $31/12/1959 = 2\pi \times$	Daily variation $= 2\pi \times$
ℓ_1	0.9406 5442 8812 5000	+ 0.5652 4720 1208 3333
ℓ_2	0.0427 5197 0477 7778	+ 0.2815 9656 0200 0000
ℓ_3	0.3438 0071 0875 0000	+ 0.1397 7123 9694 4444
ℓ_4	0.7025 5215 8347 2222	+ 0.0599 1974 8972 2222
π_1	0.3517 7383 1250 0000	+ 0.0004 3870 9722 2222
π_2	0.4138 9361 2777 7778	+ 0.0001 3087 6666 6667
π_3	0.3694 6197 9305 5556	+ 0.0000 1930 9166 6667
π_4	0.9023 3018 4027 7778	+ 0.0000 0527 0833 3333
ω_1	0.9339 4899 5138 8889	− 0.0003 7230 6944 4444
ω_2	0.8166 4930 4027 7778	− 0.0000 9083 1388 8889
ω_3	0.4661 1489 5555 5556	− 0.0000 1938 2222 2222
ω_4	0.9135 1122 8055 5556	− 0.0000 0487 6111 1111
ψ	0.8801 0470 7361 1111	+ 0.0000 0009 9722 2222
G	0.6840 6586 4444 4444	+ 0.0002 3080 8888 8889
G	0.5249 4424 2500 0000	+ 0.0000 9294 3888 8889
Π	0.0392 7971 0277 7778	+ 0.0000 0010 6111 1111

For accurate computations, argument G should be supplemented in each of its occurrences by the long period correction:

$$2\pi [0.9500\ 0000 \times 10^{-4} \sin 2\pi(0.3696\ 5917 - 0.4492\ 1389 \times 10^{-4} [t - 1960.0]_{days})$$

$$+ 0.9208\ 3333 \times 10^{-3} \sin 2\pi(0.4361\ 4306 + 0.2927\ 7778 \times 10^{-5} [t - 1960.0]_{days})]$$

Positions of Equatorial and Orbital Planes

ξ_i, η_i: In Sampson's coordinate system, the first two components of a vector of modulus 1, perpendicular to the mean orbital plane of the ith satellite (for $i = 1, 2, 3, 4$) or Jupiter's equatorial plane (for $i = 0$).

$$\xi_i \times 10^6 = \Sigma A \sin \alpha, \quad \eta_i \times 10^6 = \Sigma(-A) \cos \alpha$$

the coefficients A and the arguments α being:

i	A	α	i	A	α
0	+ 54 140	ψ	3	+ 52 623	ψ
				+ 3 106	ω_3
1	+ 54 109	ψ		+ 608	ω_4
	+ 475	ω_1		− 279	ω_2
	+ 176	ω_2		+ 32	$2G + 2\Pi - \psi$
	+ 37	ω_3		+ 6	$\psi - G$
	+ 10	ω_4		− 4	$\psi + G$
2	+ 53 843	ψ	4	+ 46 661	ψ
	+ 8 137	ω_2		+ 4 739	ω_4
	+ 436	ω_3		− 517	ω_3
	+ 103	ω_4		+ 77	$2G + 2\Pi - \psi$
	− 25	$4\ell_2 - 2\ell_1 - \omega_2$		− 38	$2\Pi - \psi$
	− 14	ω_1		+ 11	$\psi - G$
	+ 14	$2G + 2\Pi - \psi$		− 10	$\psi + G$
				+ 9	$3G + 2\Pi - \psi$

Equatorial True Longitudes

For the ith satellite, we have:

$$v_i = \ell_i + 2\pi \times 10^{-8} \cdot \Sigma A \sin \alpha$$

with the following values for A and expressions for α :

A	α	A	α	A	α
FIRST SATELLITE					
$-\ 1\ 097$	$\ell_1 - \ell_2$	$+\quad 39$	$3\ell_1 - 3\ell_3$	$-\ 431$	G
$+130\ 978$	$2\ell_1 - 2\ell_2$	$+\quad 6$	$4\ell_1 - 4\ell_3$	$+\quad 97$	$2G$
$+\quad 439$	$3\ell_1 - 3\ell_2$	$+\ 1\ 478$	$\ell_1 - \pi_1$	$-\ 206$	$\psi - \omega_1$
$+\quad 431$	$4\ell_1 - 4\ell_2$	$+\ 1\ 183$	$\ell_1 - \pi_3$	$+\quad 56$	$\psi - \omega_2$
$+\quad 33$	$5\ell_1 - 5\ell_2$	$+\quad 528$	$\ell_1 - \pi_4$	$+\ 214$	$\psi - \omega_2$
$+\quad 14$	$6\ell_1 - 6\ell_2$	$-\ 2\ 000$	$\ell_2 - 2\ell_3 + \pi_1$	$-\quad 97$	$\psi - \omega_4$
$+\quad 6$	$7\ell_1 - 7\ell_2$	$+\ 1\ 094$	$\ell_2 - 2\ell_3 + \pi_2$	$+\ 267$	$\omega_2 - \omega_3$
$-\quad 439$	$\ell_1 - \ell_3$	$+\ 2\ 517$	$\ell_2 - 2\ell_3 + \pi_3$		
$+\quad 369$	$2\ell_1 - 2\ell_3$	$+\quad 983$	$\ell_2 - 2\ell_3 + \pi_4$		
SECOND SATELLITE					
$-\ 3\ 283$	$\ell_2 - \ell_3$	$+\ 2\ 625$	$\ell_2 - \pi_2$	$+\quad 94$	$2\ell_3 - 2G - 2\Pi$
$+297\ 267$	$2\ell_2 - 2\ell_3$	$+\ 9\ 794$	$\ell_2 - \pi_3$	$-2\ 908$	G
$+\ 1\ 333$	$3\ell_2 - 3\ell_3$	$+\ 4\ 119$	$\ell_2 - \pi_4$	$-\ 325$	$2G$
$+\ 1\ 503$	$4\ell_2 - 4\ell_3$	$+\ 3\ 169$	$\ell_2 - 2\ell_3 + \pi_1$	$-\ 236$	$5G' - 2G + 48°.6$
$+\quad 106$	$5\ell_2 - 5\ell_3$	$+\ 2\ 125$	$\ell_2 - 2\ell_3 + \pi_2$	$+\ 128$	$\pi_3 - \pi_4$
$+\quad 150$	$6\ell_2 - 6\ell_3$	$-12\ 375$	$\ell_2 - 2\ell_3 + \pi_3$	$-3\ 514$	$\psi - \omega_2$
$+\quad 19$	$7\ell_2 - 7\ell_3$	$-\ 4\ 994$	$\ell_2 - 2\ell_3 + \pi_4$	$-\ 544$	$\psi - \omega_3$
$-\quad 181$	$\ell_2 - \ell_4$	$+\quad 86$	$3\ell_2 - 2\ell_3 - \pi_3$	$+\ 256$	$\psi - \omega_4$
$+\quad 125$	$2\ell_2 - 2\ell_4$	$-\quad 75$	$3\ell_2 - 4\ell_3 + \pi_2$	$+\quad 92$	$\omega_2 - \omega_3$
$+\quad 14$	$3\ell_2 - 3\ell_4$	$+\quad 553$	$3\ell_2 - 4\ell_3 + \pi_3$	$+\ 156$	$\omega_3 - \omega_4$
$+\quad 256$	$\ell_2 - \pi_1$	$+\quad 231$	$3\ell_2 - 4\ell_3 + \pi_4$		

Equatorial True Longitudes (Cont.)

A	α	A	α	A	α
		THIRD SATELLITE			
-19 161	$\ell_2 - \ell_3$	- 83	$\ell_3 - \pi_2$	+ 814	$\ell_2 - 2\ell_3 + \pi_4$
- 303	$2\ell_2 - 2\ell_3$	+48 289	$\ell_3 - \pi_3$	-3 736	G
- 333	$3\ell_2 - 3\ell_3$	+ 47	$2\ell_3 - 2\pi_3$	- 114	2G
- 19	$4\ell_2 - 4\ell_3$	+20 492	$\ell_3 - \pi_4$	- 331	$5G' - 2G + 48°.6$
- 8	$5\ell_2 - 5\ell_3$	- 217	$2\ell_2 - 3\ell_3 + \pi_3$	+ 192	$\pi_3 - \pi_4$
- 11	$6\ell_2 - 6\ell_3$	- 97	$2\ell_2 - 3\ell_3 + \pi_4$	+ 122	$\psi - \omega_2$
- 1 192	$\ell_3 - \ell_4$	+ 150	$\ell_3 - 2G - 2\Pi + \pi_3$	-1 867	$\psi - \omega_3$
+ 4 075	$2\ell_3 - 2\ell_4$	- 1 678	$\ell_3 - 2\ell_4 + \pi_4$	+ 167	$\psi - \omega_4$
+ 286	$3\ell_3 - 3\ell_4$	- 100	$\ell_2 - 2\ell_3 + \pi_1$	+ 267	$\omega_3 - \omega_4$
+ 67	$4\ell_3 - 4\ell_4$	- 922	$\ell_2 - 2\ell_3 + \pi_2$		
+ 19	$5\ell_3 - 5\ell_4$	+ 1 869	$\ell_2 - 2\ell_3 + \pi_3$		
		FOURTH SATELLITE			
+ 161	$\ell_1 - \ell_4$	- 5 775	$\ell_4 - \pi_3$	-8 933	G
+ 142	$2\ell_1 - 2\ell_4$	+234 697	$\ell_4 - \pi_4$	- 322	2G
- 636	$\ell_3 - \ell_4$	+ 1 078	$2\ell_4 - 2\pi_4$	+ 100	$2G' - G + 173°.17$
- 319	$2\ell_3 - 2\ell_4$	+ 278	$\ell_3 - 2\ell_4 + \pi_4$	- 781	$5G' - 2G + 48°.64$
- 69	$3\ell_3 - 3\ell_4$	+ 358*	$2\ell_4 - 2G - 2\Pi$	+ 222	$\psi - \omega_3$
- 19	$4\ell_3 - 4\ell_4$	+ 1 764	$\ell_4 - 2G - 2\Pi + \pi_4$	- 556	$\psi - \omega_4$

* H. Andoyer [Bull. Astr. 32, 1915] gives the corrected value + 386 for this coefficient.

Radii Vectors

(projected on the equator)
(in astronomical units of length)

$r_1 \times 10^9 = 2.819\ 55\ [10^6\ +$ $20\ \cos\ (\ell_1 - \ell_2)$ $- 4125\ \cos\ (2\ell_1 - 2\ell_2)$ $- 20\ \cos\ (3\ell_1 - 3\ell_2)$ $- 15\ \cos\ (4\ell_1 - 4\ell_2)$ $+ 10\ \cos\ (\ell_1 - \ell_3)$ $- 15\ \cos\ (2\ell_1 - 2\ell_3)$ $- 45\ \cos\ (\ell_1 - \pi_1)$ $- 35\ \cos\ (\ell_4 - \pi_3)$ $- 15\ \cos\ (\ell_1 - \pi_4)]$	$r_2 \times 10^9 = 4.486\ 12\ \ [10^6\ +$ $55\ \cos\ (\ell_2 - \ell_3)$ $- 9430\ \cos\ (2\ell_2 - 2\ell_3)$ $- 55\ \cos\ (3\ell_2 - 3\ell_3)$ $- 30\ \cos\ (4\ell_2 - 4\ell_3)$ $- 85\ \cos\ (\ell_2 - \pi_2)$ $- 310\ \cos\ (\ell_2 - \pi_3)$ $- 130\ \cos\ (\ell_2 - \pi_4)]$
$r_3 \times 10^9 = 7.155\ 87\ [10^6\ +$ $635\ \cos\ (\ell_2 - \ell_3)$ $+ 15\ \cos\ (2\ell_2 - 2\ell_3)$ $- 15\ \cos\ (3\ell_2 - 3\ell_3)$ $+ 25\ \cos\ (\ell_3 - \ell_4)$ $- 140\ \cos\ (2\ell_3 - 2\ell_4)$ $- 10\ \cos\ (3\ell_3 - 3\ell_4)$ $- 1515\ \cos\ (\ell_3 - \pi_3)$ $- 645\ \cos\ (\ell_3 - \pi_4)]$	$r_4 \times 10^9 = 12.586\ 25\ \ [10^6\ +$ $100\ \cos\ (\ell_3 - \ell_4)$ $+ 20\ \cos\ (2\ell_3 - 2\ell_4)$ $+ 180\ \cos\ (\ell_4 - \pi_3)$ $- 7375\ \cos\ (\ell_4 - \pi_4)$ $- 25\ \cos\ (2\ell_4 - 2\pi_4)$ $- 55\ \cos\ (\ell_4 - 2G - 2\Pi + \pi_4)]$

Additional Terms of the Longitudes in Sampson's System

Let $\Delta v_i = 2\pi \times 10^{-8} \Sigma\, A \sin\, \alpha$ (rad) be the correction to be added to v_i in order to obtain the true longitude of ith satellite in Sampson's co-ordinate system.

i	A	α
1	$-11\ 667$	$2\ell_1 - 2\psi$
	$-\ \ \ \ 206$	$2\ell_1 - \psi - \omega_1$
	$-\ \ \ \ \ 78$	$2\ell_1 - \psi - \omega_2$
2	$-11\ 553$	$2\ell_2 - 2\psi$
	$-\ \ 3\ 514$	$2\ell_2 - \psi - \omega_2$
	$-\ \ \ \ 186$	$2\ell_2 - \psi - \omega_3$
	$-\ \ \ \ \ 44$	$2\ell_2 - \psi - \omega_4$
	$-\ \ \ \ 267$	$2\ell_2 - 2\omega_2$
3	$-11\ 025$	$2\ell_3 - 2\psi$
	$+\ \ \ \ 122$	$2\ell_3 - \psi - \omega_2$
	$-\ \ 1\ 303$	$2\ell_3 - \psi - \omega_3$
	$-\ \ \ \ 264$	$2\ell_3 - \psi - \omega_4$
4	$-18\ 661$	$2\ell_4 - 2\psi$
	$-\ \ 1\ 781$	$2\ell_4 - \psi - \omega_4$
	$+\ \ \ \ 189$	$2\ell_4 - \psi - \omega_3$
	$-\ \ \ \ \ 83$	$2\ell_4 - 2\omega_4$
	$-\ \ \ \ \ 28^*$	$2\ell_4 - 2G - 2\pi$

* Only to be introduced if H. Andoyer's correction in the equatorial longitude is adopted.

N. B. To obtain full-accuracy determinations of the positions, v_i should be substituted to ℓ_i in the arguments α.

Latitude Series

b_i being the latitude of the ith satellite, relative to Sampson's (x, y)-plane:

$$\operatorname{tg} b_i = 10^{-7} \Sigma \, B \sin \beta$$

i	B	β	i	B	β
1	+ 541 683	$\ell_1 - \psi$	3	+ 526 783	$\ell_3 - \psi$
	− 192	$3\ell_1 - 3\psi$		− 181	$3\ell_3 - 3\psi*$
	+ 4 759	$\ell_1 - \omega_1$		+ 31 126	$\ell_3 - \omega_3$
	+ 1 757	$\ell_1 - \omega_2$		− 2 792	$\ell_3 - \omega_2$
	+ 367	$\ell_1 - \omega_3$		+ 6 084	$\ell_3 - \omega_4$
	+ 96	$\ell_1 - \omega_4$		+ 319	$\ell_3 + \psi - 2G - 2\Pi$
2	+ 539 020	$\ell_2 - \psi$		+ 56	$\ell_3 - \psi + G$
	− 200	$3\ell_2 - 3\psi$		− 44	$\ell_2 - \psi - G$
	+ 81 549	$\ell_2 - \omega_2$	4	+ 466 987	$\ell_4 - \psi$
	− 140	$\ell_2 - \omega_1$		− 128	$3\ell_4 - 3\psi$
	+ 4 362	$\ell_2 - \omega_3$		− 384	$\ell_4 + \psi - 2\Pi$
	+ 1 028	$\ell_2 - \omega_4$		+ 47 471	$\ell_4 - \omega_4$
	− 250	$2\ell_1 - 3\ell_2 + \omega_2$		− 5 171	$\ell_4 - \omega_3$
	+ 140	$\ell_2 + \psi - 2G - 2\Pi$		+ 767	$\ell_4 + \psi - 2G - 2\Pi$
	+ 90	$\ell_2 - 2\psi + \omega_2$		+ 89	$\ell_4 + \psi - 3G - 2\Pi$
	− 90	$3\ell_2 - 2\psi - \omega_2$		+ 107	$\ell_4 - \psi + G$
				− 103	$\ell_4 - \psi - G$

*Erroneously $3\ell_4 - 3\psi$ in Sampson's Tables.

N.B. To obtain full accuracy determinations of the positions, v_i should be substituted to ℓ_i in the arguments β!

BIBLIOGRAPHY

1. Battin, Richard H., "Astronautical Guidance," McGraw-Hill Book Company, 1964.

2. Escobal, Pedro R., "Methods of Orbit Determination," John Wiley and Sons, 1965.

3. Nelson, Walter C., Loft, Ernest E., "Space Mechanics" Prentice Hall, Inc., 1962.

4. Danby, J. M. A., "Fundamentals of Celestial Mechanics," MacMillan Company, 1964.

5. Baker, R. M. L.; Makemson, M. W., "An Introduction to Astrodynamics," Academic Press, 1960.

6. Battin, R. H., "The Determination of Round-Trip Planetary Reconnaissance Trajectories," J. Aerospace Science, Volume 26, pp. 545-567, September, 1959.

7. "Programmer's Manual for Quick Look Mission Analysis Program," Philco, WDL Division, WDL-TR2217, Contract NAS 5-3342, January 1964.

8. Kaufman, B; Newman, C. R., Chromey, F., "Gravity Assist Optimization Technique Applicable to a Variety of Space Missions," GSFC Document X-507-66-373, August 1966.

9. Newman, C. R.; Kaufman, B., "The Effects of Jovian Encounter Geometry on the Post-Encounter Heliocentric Trajectory." GSFC Document to be published.

10. Minovitch, M. A., "The Determination and Characteristics of Ballistic Interplanetary Trajectories Under the Influence of Multiple Planetary Attractions," JPL Technical Report No. 32-464, October 31, 1963.

66

11. Minovitch, M. A., "Utilizing Large Planetary Perturbations for the Design of Deep-Space, Solar Probe, and Out-of-Ecliptic Trajectories," JPL Technical Report No. 32-849, December 15, 1965.

12. Porter, R. F., Luce, R. G.; Edgecombe, D. S., "Gravity-Assisted Trajectories for Unmanned Space Exploration," Battelle Memorial Institute Report No. BM-NLVP-FTR-65-1, September 23, 1965.

13. Niehoff, John C., "An Analysis of Gravity Assisted Trajectories to Solar System Targets," IIT Research Institute, AIAA Paper No. 66-10, January 1966.

14. Vonbun, F. O., "Transfer Geometry, Communications Conditions and Definitions for Galactic Probe Analysis," Mission Analysis Office Technical Study, Goddard Space Flight Center, October 4, 1965.

15. Sturms, F. M., Jr., "Trajectory Analysis of an Earth-Venus-Mercury Mission in 1973," JPL Technical Report No. 32-1062, January 1, 1967.

16. Herget, Paul, "A Device in Satellite Perturbation Computations", Astronomical Journal, No. 1162 pp. 177-178, 1946.

17. Linnekin, Jerry S., Belliveau, L. J., "FNOL 2, A Fortran (IBM 7090) Subroutine for the Solution of Ordinary Differential Equations with Automatic Adjustment of the Interval of Integration," U.S. Naval Ordinance Laboratory, NOLTR 63-171, July 17, 1963.

18. "Wanderers in the Sky," Edited by Thornton Page and Lou Williams Page, Macmillan Co., N. Y., 1965.

19. Baker, Robert H., "Astronomy," D. Van Nostrand Co, Inc. 1964.

20. "Space Facts" Compiled and published by the General Electric Missile and Space Vehicle Department, 1960.

21. Michaux, C. M., "Handbook of the Physical Properties of the Planet Jupiter," Douglas Aircraft Company, NASA contract publication, NASA SP-3031, 1967.

22. Porter, J. C., "The satellites of the Planets," J. Brit. Astron. Assoc., Vol. 70, No. 1, January 1931.

23. Sampson, R. A., "Tables of the Four Great Satellites of Jupiter," University of Durham Observatory, William Wesley and Son, 1910.

24. Sampson, R. A., "Theory of the Four Great Satellites of Jupiter," Publication of the Royal Astronomical Society, Vol. LXIII, 1920.

25. De Sitter, W., "Jupiter's Galilean Satellites," Monthly Notices Roy. Astron, Soc., Vol. 91, No. 7, May 1931.

26. "Explanatory Supplement to the Ephemeris," Prepared Jointly by the Nautical Almanac Offices of the United Kingdom and the U.S.; Her Majesty's Stationary Office, 1961.

27. Andoyer, H., "Sur le Calcul des Ephe'merides des Quatre Anciens Satellites de Jupiter," Bulletin Astronomique, 32, 177, 1915.

28. Mello, Ferraz S., Bull. Astr., (3), Vol. 1, fasc. 4, 1966.

29. Marsden, B. G., "The Motion of the Galilean Satellites of Jupiter," Dissertation, Yale University, 1966.

30. Private Communication with Dr. Jean L. Sagnier, Bureau des Longitudes, Palais de L'Institute, Paris, France.

31. Coady, Robert E., "Trajectory Analysis - Near-Earth and Jupiter-Approach Phases of the 1972 Galactic Jupiter Probe Mission," Mission Analysis Office Technical Study, Goddard Space Flight Center, April 28, 1967.